

# Rigid-Rod $\beta$ -Barrels as Lipocalin Models: Probing Confined Space by Carotenoid Encapsulation

Bodo Baumeister<sup>[a]</sup> and Stefan Matile\*<sup>[a, b]</sup>

**Abstract:** Herein, we describe the design, synthesis, structure, and function of synthetic, supramolecular  $\beta$ -barrel models. Assembly of octi(*p*-phenylene)s with complementary -Lys-Leu-Lys-NH<sub>2</sub> and -Glu-Leu-Glu-NH<sub>2</sub> side chains yielded water-soluble rigid-rod  $\beta$ -barrels of precise length and with flexible diameter. A hydrophobic interior was evidenced by

guest encapsulation. Host-guest complexes with planarized, monomeric  $\beta$ -carotene within tetrameric rigid-rod  $\beta$ -barrels, and disc micellar astaxanthin

**Keywords:** bioorganic chemistry • cage compounds • carotenoids • oligomers • peptidomimetics

J-aggregates surrounded by about dodecameric rigid-rod “bicycle tires” were prepared from mixed micelles by dialytic detergent removal. The significance of these findings for future bioorganic chemistry in confined, intratoroidal space is discussed in comparison with pertinent biological examples.

## Introduction

Toroidal structures are ubiquitous in nature.<sup>[1–9]</sup> With respect to their remarkable functional diversity, the confined interior of toroidal structures is of particular interest. For instance, there is mounting evidence that the large protein assemblies of molecular machines utilize intratoroidal space to mediate macromolecular processes such as protein folding,<sup>[1]</sup> protein degradation,<sup>[2]</sup> oligonucleotide binding,<sup>[3]</sup> and gene replication.<sup>[4]</sup> Among other examples, the mediation of molecular transport across cell membranes by various membrane proteins on the one hand<sup>[5]</sup> and binding of hydrophobic natural products by lipocalins on the other<sup>[6–9]</sup> illustrate biological functionality of both hydrophilic and hydrophobic confined intratoroidal cores.

In nature, confined interiors are often created by  $\beta$ -barrels.<sup>[1–9]</sup> In order to examine the uniqueness of intratoroidal chemistry beyond the limitations of peptide chemistry, we recently focused our attention on the development of artificial  $\beta$ -barrels.<sup>[10]</sup> A general strategy for the design of supramolecular rigid-rod  $\beta$ -barrels has been implied by LaBrenz and Kelly’s pioneering study with dibenzofuran peptide **1**.<sup>[11]</sup> This artificial receptor binds the complementary peptide **2** by forming antiparallel  $\beta$ -sheets with interdigitating peptide strands in host-guest complex **3** (Figure 1).<sup>[11]</sup> Com-

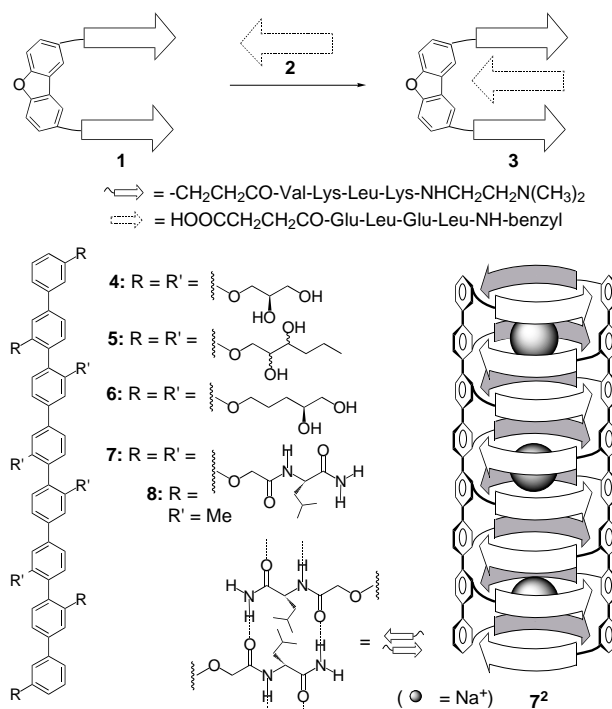


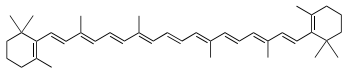
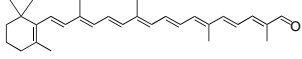
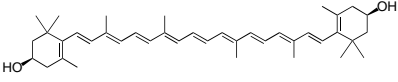
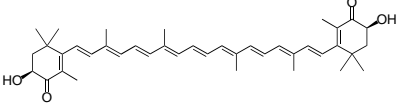
Figure 1. Structures of LaBrenz and Kelly’s model **3**, rigid-rod polyols **4–6**, and self-assembled rigid-rod  $\beta$ -barrel **7**.<sup>[10–12]</sup>

[a] Prof. Dr. S. Matile, Dipl.-Chem. B. Baumeister  
 Department of Organic Chemistry, University of Geneva  
 1211 Geneva 4 (Switzerland)  
 Fax: (+41) 22-328-7396  
 E-mail: stefan.matile@chiorg.unige.ch

[b] Prof. Dr. S. Matile  
 Department of Chemistry, Georgetown University  
 Washington, DC 20057 (USA)

parable antiparallel strand interdigitations were observed in our laboratory during the study of rigid-rod ion-channel models **4–8**.<sup>[10, 12]</sup> Rigid-rod polyol **4**<sup>[12f, g]</sup> (but not the more flexible **5** and **6**)<sup>[12e]</sup> was initially suspected to form transient toroidal supramolecules in highly polarized black lipid membranes.<sup>[12d]</sup> To obtain permanently stable rigid-rod  $\beta$ -

Table 1. Characteristics of carotenoid encapsulation.

Entry	carotenoid <sup>[a]</sup>	Starting materials		Products						
		$\lambda$ [nm] <sup>[b]</sup>	<b>13</b> <sup>[c]</sup>	<b>14</b> <sup>[d]</sup>	yield [%] <sup>[e]</sup>	$\lambda$ [nm] <sup>[f]</sup>	GF (SEC) <sup>[g]</sup>	$x$ <sup>[h]</sup>	FQ [%] <sup>[i]</sup>	
1		<b>11</b>	436	0.5	0.5	25 <sup>[j]</sup>	480	+ (+)	4:1	48
2		<b>11</b>	436	0	0	— <sup>[k]</sup>				
3		<b>11</b>	436	0	0	—				
4		<b>18</b>	446	0.5	0.5	—				
5		<b>18</b>	446	0	0	18	464			
6		<b>9</b>	450	0.25	0.25	—				
7		<b>9</b>	450	0	0.5	40	388 (450) <sup>[l]</sup>			
8		<b>9</b>	450	0	0	36	388 (450) <sup>[l]</sup>			
9		<b>10</b>	445	0.1	0.1	10	576	+ (-)	1:1	29
10		<b>10</b>	445	0	0.2	6	560 (524)	—		
11		<b>10</b>	445	0	0	17	560 (524)	—		

[a] **9**: zeaxanthin; **10**: astaxanthin; **11**:  $\beta$ -carotene; **18**:  $\beta$ -apo-8'-carotenal. [b] Absorption maxima of carotenoid in mixed cholate micelles. [c] [**13**]/[carotenoid]. [d] [**14**]/[carotenoid]. [e] Determined by carotenoid absorption after dialysis and filtration. [f] Absorption maxima of isolated carotenoid in buffer, pH 6.4; significant maxima of fine structure are given in parenthesis. [g] GF: Gel filtration (SEC: Size exclusion chromatography). [h]  $x$  = stoichiometry oligo(*p*-phenylene)/carotenoid (determined by spectroscopy). [i] FQ: Quenching of oligo(*p*-phenylene) fluorescence. [j] Quantitative with respect to oligo(*p*-phenylene) concentration. [k] Yields < 5% were not considered. [l] Relative intensity of the two maxima was concentration dependent as in ref. [18].

barrels, we subsequently replaced the lateral glycol side chains in **4** by the lateral diamides in **7**.<sup>[10]</sup> The resulting dimer **7** was stable in polar and nonpolar solvents.<sup>[10]</sup> The lack of similar self-organization of octi(*p*-phenylene) **8** with four instead of eight lateral diamide chains demonstrated the importance of multiple intermolecular interactions along the preorganizing rigid-rod scaffold for molecular architecture.<sup>[10]</sup>

Self-assembled rigid-rod  $\beta$ -barrel **7** contains a lipophilic surface and hydrophilic intratoroidal space for multiple cation binding, that is, toroidal amphiphilicity suitable for transmembrane ion transport.<sup>[5, 10]</sup> In the present study, we focus on both inversion of the above toroidal amphiphilicity and

expansion of rigid-rod  $\beta$ -barrels, that is, on rigid-rod lipocalin models.

Lipocalins are relatively small proteins associated with pheromone activity, invertebrate coloration, olfaction, and gustation and have an eight-stranded antiparallel  $\beta$ -barrel in common.<sup>[6–9]</sup> Lipocalins are attracting increasing attention as universal ligand-binding proteins, a feature considered as unique for immunoglobulins until recently.<sup>[6]</sup> Among lipocalins, carotenoproteins were of particular interest for the present study.<sup>[7, 8]</sup> Photoprotective xanthophyll-cycle enzymes that catalyze epoxidation and de-epoxidation of zeaxanthin **9** and violaxanthin, respectively, were identified as lipocalins with intratoroidal carotenoid binding-sites up to 40 Å deep (see Table 1 for carotenoid structures).<sup>[7]</sup> The classical carotenoproteins from the lobster carapace that account for its characteristic blue color, crustacyanins, are composed of lipocalin heterodimers with two internal astaxanthins **10**.<sup>[8]</sup> A comparable case was reported for  $\beta$ -lactoglobulin, a lipocalin abundant in milk that binds and stabilizes one vitamin A per  $\beta$ -barrel.<sup>[9]</sup>

The dependence of the spectroscopic properties of carotenoids on their local environment identified these chromophores as superb, hydrophobically matching probes for the interior of rigid-rod  $\beta$ -barrels.<sup>[13–18]</sup> Because of its significance in photosynthetic systems, the spectroscopic properties of  $\beta$ -carotene **11** in particular have been studied in detail.<sup>[13–17]</sup> The  $S_0 \rightarrow S_2$  transition of  $\beta$ -carotene shows a hypsochromic shift with increasing solvent polarity.<sup>[13]</sup> Practically no shifts but loss of vibronic fine structure plus strong exciton coupled circular dichroism (CD) were reported for  $\beta$ -carotene aggregates in chiral environments such as lipid bilayers<sup>[14c]</sup> or reconstituted low-density lipoprotein capsules.<sup>[14b]</sup> An increase in vibronic

**Abstract in French:** *Nous décrivons la conception, la synthèse, la structure et la fonction de modèles supramoléculaires et synthétiques pour des barriques  $\beta$ . L'assemblage des octa(*p*-phenylène)s complémentaires avec les chaînes latérales -Lys-Leu-Lys-NH<sub>2</sub> et -Glu-Leu-Glu-NH<sub>2</sub> a donné des barriques  $\beta$  faites de «baguettes moléculaires» qui sont caractérisées par une longueur précise, un diamètre flexible, et une solubilité dans l'eau. L'intérieur hydrophobe a été prouvé par encapsulation de substrats. Des complexes substrat-récepteur avec un  $\beta$ -carotène planarisé dans une barrique  $\beta$  tétramérique, et des disques micellaires composés d'agrégats J de l'astaxanthine entourés par des «pneus de vélo» faits par—probablement douze—«baguettes» ont été préparés à partir de micelles mixtes en enlevant les détergents par dialyse. L'importance de ces découvertes pour une future chimie bioorganique dans l'espace confiné intratoroidal est discutée en comparaison avec des exemples pertinents de la biologie.*

fine structure together with a bathochromic shift has been found at low temperature,<sup>[15]</sup> in single crystals,<sup>[16]</sup> and upon ring–chain co-planarization.<sup>[9, 17]</sup> The most striking spectroscopic features of carotenoids other than  $\beta$ -carotene include a strong blue-shift of zeaxanthin and astaxanthin upon aggregation.<sup>[18]</sup> On the other hand, a bathochromic effect has been found for lipocalin-bound astaxanthin<sup>[8]</sup> that may be comparable to the opsin shift underlying the chemistry of vision.<sup>[19]</sup> Thus, the spectroscopic properties of carotenoids encapsulated by hydrophobically matching rigid-rod  $\beta$ -barrels are likely to reveal the nature of their interior.

In the following, we describe the design, synthesis, and structure of supramolecular rigid-rod  $\beta$ -barrels **12<sup>4</sup>** and **12<sup>6</sup>** (Figure 2). We also report encapsulation of  $\beta$ -carotene and astaxanthin by these artificial lipocalins, and structural studies of the resulting host–guest complexes.

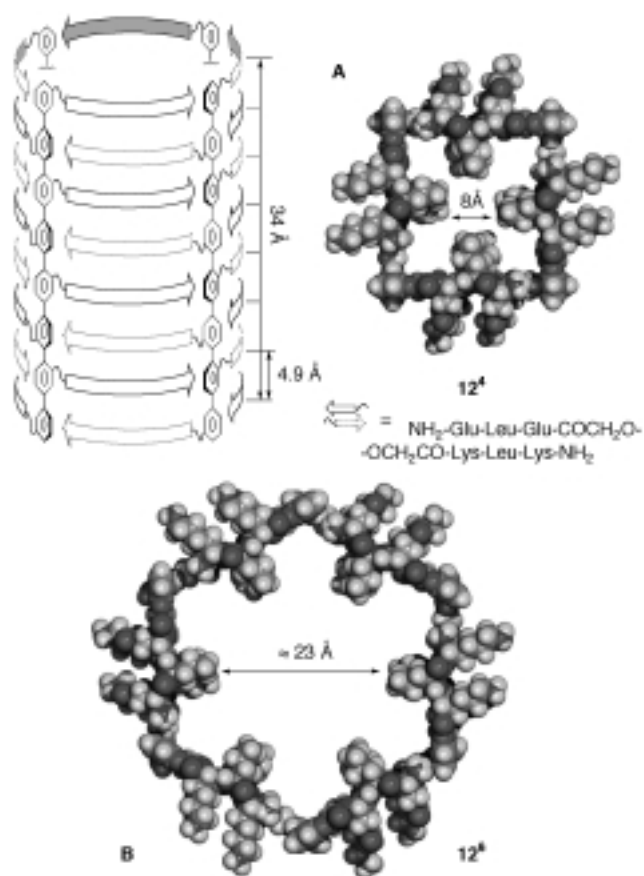


Figure 2. Molecular architecture of rigid-rod  $\beta$ -barrels. Schematic side view of tetramer **12<sup>4</sup>** and top view of molecular models of **12<sup>4</sup>** (A) and hexamer **12<sup>6</sup>** (B); only the two top strands are shown for clarity. Molecular modeling was done with Cerius2 (Molecular Simulations) and Insight II/Discover (BIOSYM Technologies).

## Results and Discussion

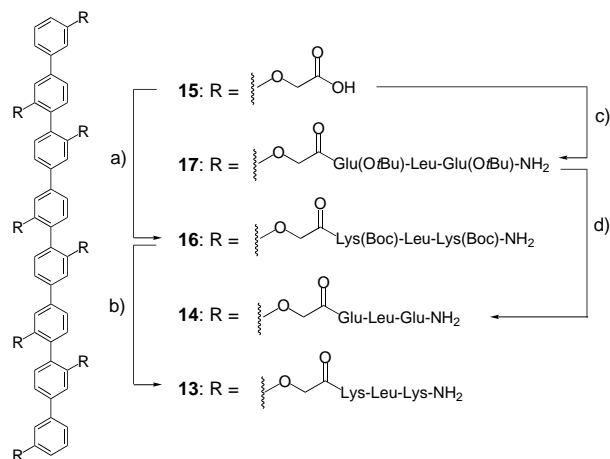
**Design and molecular modeling of rigid-rod  $\beta$ -barrels:** Rigid-rod  $\beta$ -barrels **12<sup>n</sup>** were designed based on the following considerations:

1. Rigid-rod scaffolds were selected to preorganize the interdigitation of peptide strands, as in rigid-rod  $\beta$ -barrel

**7<sup>2</sup>**.<sup>[10]</sup> The length of an octi(*p*-phenylene) scaffold is practically identical to that of an eight-stranded  $\beta$ -sheet (Figure 2).

- Spontaneous self-assembly has been identified as a major limitation of rigid-rod  $\beta$ -barrel **7<sup>2</sup>** for several reasons, which include purification of the target molecule, access to thermodynamic data, and guest encapsulation. Control over the assembly of rigid-rod  $\beta$ -barrels **12<sup>n</sup>** by using, in analogy to LaBrenz and Kelly's model **3**,<sup>[11]</sup> two rigid-rod molecules with complementary lateral peptides was thus desirable.
- Charged lateral side chains are advantageous to ascertain solubility in water, to prevent spontaneous intra- and intermolecular side chain interactions in the absence of the complementary rod, and for constructive electrostatic interactions upon peptide-strand interdigitation.
- Hydrophobic amino acid residues alternating with charged ones are needed to create the hydrophobic interior upon  $\beta$ -barrel formation in water.

The polycationic Lys-Leu-Lys-rod **13** and the complementary polyanionic Glu-Leu-Glu-rod **14** fulfill these prerequisites (Scheme 1).



Scheme 1. a) H-Lys(Boc)-Leu-Lys(Boc)-NH<sub>2</sub>, PyBOP, DIPEA, 2 h, 57%; b) TFA/CH<sub>2</sub>Cl<sub>2</sub>, 5 min, quantitative; c) H-Glu(OtBu)-Leu-Glu(OtBu)-NH<sub>2</sub>, PyBOP, DIPEA, 2 h, 57%; d) TFA/CH<sub>2</sub>Cl<sub>2</sub>, 45 min, quantitative.

Molecular models of rigid-rod supramolecules **12<sup>n</sup>** composed of **13** and **14** revealed  $\beta$ -barrels with lipocalin-type toroidal amphiphilicity, precisely defined length, and a flexible diameter (Figure 2A and B). This architecture is opposite to that of thoroughly investigated nanotubes with fixed diameter and flexible length formed by stacked cyclic peptides, carbohydrates, and phenylacetylenes.<sup>[20]</sup> Flexibility in internal diameter, however, seems essential for the encapsulation of hydrophobic guests of different volume.

Three clearly distinct situations were identified by molecular modeling of **12<sup>n</sup>**. Dimeric supramolecules with an architecture analogous to that of self-assembled ionophore **7<sup>2</sup>** (Figure 1) could not be assembled because of the steric demand of the intratoroidal Leu-residues (not shown). The same was true for the electrostatically disfavored intramolecular  $\beta$ -sheet formation in monomeric **13** and **14** (not shown).

In tetramer **12<sup>4</sup>**, the Leu-residues pointing towards the center of the  $\beta$ -barrel create a central hydrophobic channel of about 8 Å diameter with four adjacent peripheral pockets (Figure 2A). The central tube seems well preorganized to accommodate one rod-shaped, hydrophobic guest of up to 34 Å length; this guest can be firmly clamped by the four internal Leu side-chain iso-butyl arrays through multiple hydrophobic interactions.

In hexamer **12<sup>6</sup>**, the “innermolecular” space is significantly enlarged and less structured (Figure 2B). In sharp contrast to tetramer **12<sup>4</sup>**, hexamer **12<sup>6</sup>** can encompass disc micelles rather than encapsulate monomeric guests. Molecular models of higher oligomers (octamer **12<sup>8</sup>**, decamer **12<sup>10</sup>**, etc.) gave expanded “bicycle tires” that resembled hexamer **12<sup>6</sup>** with respect to general appearance and potential function (not shown).

**Oligo(*p*-phenylene) synthesis:** The complementary oligo(*p*-phenylene) peptides **13** and **14** were prepared by coupling of octaacid **15** with the tripeptides H-Lys(Boc)-Leu-Lys(Boc)-NH<sub>2</sub> and H-Glu(*Or*Bu)-Leu-Glu(*Or*Bu)-NH<sub>2</sub>, respectively (Scheme 1). Tripeptides H-Lys(Boc)-Leu-Lys(Boc)-NH<sub>2</sub> and H-Glu(*Or*Bu)-Leu-Glu(*Or*Bu)-NH<sub>2</sub> were prepared by standard solution-phase peptide synthesis with Boc-protection for Lys-residues, *Or*Bu-protection for Glu-residues, and orthogonal Z-protection for the N-terminal amino function. Coupling of the final tripeptides H-Lys(Boc)-Leu-Lys(Boc)-NH<sub>2</sub> and H-Glu(*Or*Bu)-Leu-Glu(*Or*Bu)-NH<sub>2</sub> with octaacid **15** by using Py-BOP/DIPEA-methodology<sup>[21]</sup> gave rigid-rod peptides **16** and **17** in 67% and 56% yield. Peptide deprotection with TFA to give polyanion **14** and polycation **13** was quantitative. The synthesis of polyanion **14** has been previously communicated.<sup>[12a]</sup>

**Programmed assembly of rigid-rod  $\beta$ -barrels:** Size-exclusion chromatography (SEC) of an equimolar mixture of polycation **13** and complementary polyanion **14** in saline buffer (pH 6.4) revealed the presence of two suprastructures (Figure 3a). Direct comparison with the retention times of protein standards implied that the apparent molecular weight of the minor product (19%) was con-

sistent with the calculated molecular weight of hexamer **12<sup>6</sup>**, while the major product (81%) corresponded to tetramer **12<sup>4</sup>**. In the absence of the complementary polyanion **14**, polycation **13** was monomeric (Figure 3c). Self-assembly of polyanion **14** into tetrameric pinwheels **14<sup>4</sup>**, with central  $\pi$ , $\pi$ -stacked arene arrays surrounded by amphiphilic tripeptides, and its significance for nanoarchitecture has been described elsewhere (Figure 3b).<sup>[12a]</sup>

The rigid-rod  $\beta$ -barrels **12<sup>4</sup>** (**12<sup>6</sup>**) in Figure 3a formed spontaneously upon addition of concentrated **13** and **14** in methanol (e.g., 20  $\mu$ L) to saline buffer at pH 6.4 (e.g., 2 mL). The results were independent of sequence of addition and octi(*p*-phenylene) concentration. Rigid-rod  $\beta$ -barrels **12<sup>4</sup>** (**12<sup>6</sup>**) were soluble at micromolar but insoluble at millimolar concentrations.<sup>[22]</sup> About identical results were obtained by solubilization of equimolar amounts of **13** and **14** in cholate micelles followed by dialytic removal of cholate (Figure 3a). However, dialytic detergent removal from mixed *n*-octyl  $\beta$ -D-glucopyranoside/octi(*p*-phenylene) micelles yielded higher oligomers **12<sup>n</sup>** (Figure 3d,  $n \approx 26$ ). Dialytic detergent removal applied to mixed cholate/octi(*p*-phenylene)/ $\beta$ -carotene micelles gave tetramers with encapsulated  $\beta$ -carotene and traces of the corresponding hexamers and oligomers (Figure 3e, see below for discussion).

**Structural studies of rigid-rod  $\beta$ -barrels:** The position of the absorption maximum of the oligo(*p*-phenylene) <sup>1</sup>L transitions at 316 nm ( $\epsilon \approx 28.6 \text{ mM}^{-1} \text{ cm}^{-1}$ )<sup>[12f]</sup> did not significantly change during the assembly of rigid-rod  $\beta$ -barrels. The circular dichroism (CD) spectra of polycationic **13** (Figure 4, dotted

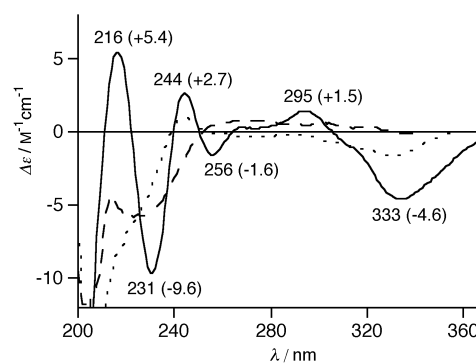


Figure 4. CD spectra of rigid-rod lipocalin **12<sup>4</sup>/12<sup>6</sup>** ( $\sim 4:1$ , solid line), rigid-rod pinwheel **14<sup>4</sup>** (dashed line), and polycation **13** (dotted line) at pH 6.4.

curve) and tetrameric pinwheel **14<sup>4</sup>** (Figure 4, dashed curve) were not distinct. These CD spectra differed clearly from that of rigid-rod  $\beta$ -barrels **12<sup>4</sup>/12<sup>6</sup>** ( $\approx 4:1$ ) in saline buffer at pH 6.4 (Figure 4, solid curve). That for **12<sup>4</sup>/12<sup>6</sup>** contains six distinct CD Cotton effects (CEs). Judged from their comparable red and blue shift from the absorption at 316 nm, the first two CE at 333 nm and 295 nm are likely to originate from exciton coupling.<sup>[10, 12b,c]</sup> Consistent with intramolecular coupling, the amplitudes seen for **12<sup>4</sup>** (**12<sup>6</sup>**) ( $A = -6.1$ ) are similar in magnitude (but opposite in sign) compared with that observed for dimer **7<sup>2</sup>** (Figure 1,  $A = +9.9$ ).<sup>[10]</sup>

The CD spectrum of **12**<sup>4</sup> (**12**<sup>6</sup>) further exhibits four high-energy CEs with increasing magnitude and alternating sign. The CEs at 231 nm ( $\Delta\epsilon = -9.6$ ) and 216 nm ( $\Delta\epsilon = +5.4$ ) are red-shifted relative to the expected values for  $\beta$ -sheets.<sup>[23–25]</sup> If the negative CE at 231 nm originates from a  $\beta$ -sheet conformation, then it indicates flattened and/or twisted  $\beta$ -sheets in **12**<sup>4</sup> (**12**<sup>6</sup>).<sup>[24]</sup> However, since additional contributions from oligo(*p*-phenylene) <sup>1</sup>B transitions were also expected in this region,<sup>[12b,c]</sup> further support for the  $\beta$ -barrel architecture of **12**<sup>4</sup> (**12**<sup>6</sup>) from the dependence of its CD spectrum on stoichiometry, ionic strength, pH, temperature, and concentration was essential (Figure 5).

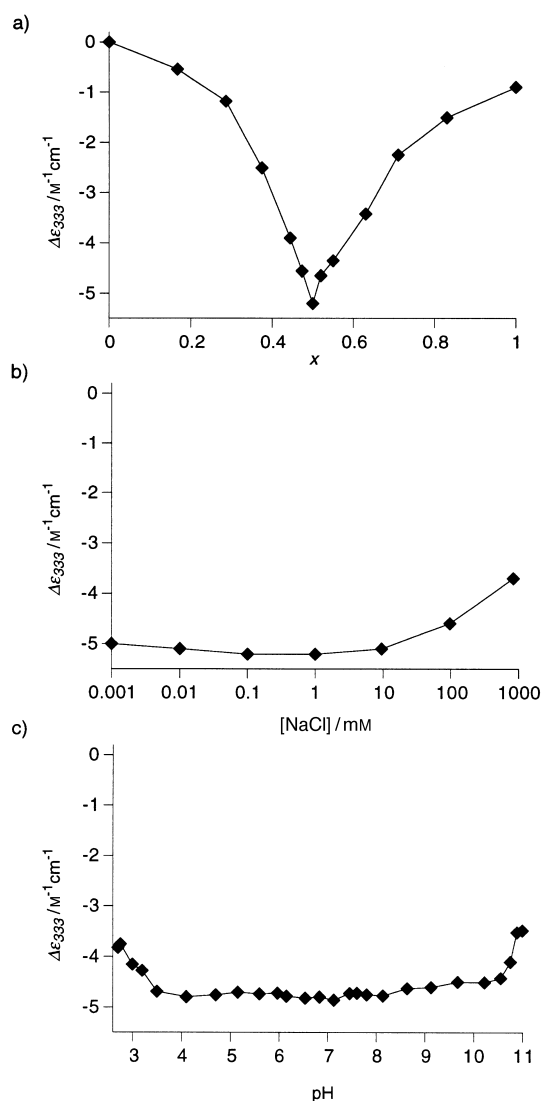


Figure 5. Dependence of the first CD Cotton effect of **12**<sup>4</sup>/**12**<sup>6</sup> (~4:1) on a) monomer stoichiometry, b) ionic strength, and c) pH. Spectra for a) were obtained in  $\text{Na}_n\text{H}_{3-n}\text{PO}_4$  (10 mM), NaCl (100 mM), pH 6.4, for b) in  $\text{Na}_n\text{H}_{3-n}\text{PO}_4$  (10 mM), pH 6.4, and for c) in  $\text{Na}_n\text{H}_{3-n}\text{PO}_4$  (10 mM), NaCl (100 mM).  $x = [\mathbf{13}]/([\mathbf{13}] + [\mathbf{14}])$ . All results were independent of the total oligo(*p*-phenylene) concentration (4–35  $\mu\text{M}$ ).

The mixing curves for rigid-rod lipocalin **12**<sup>4</sup> (**12**<sup>6</sup>) demonstrated 1:1 stoichiometry (Figure 5a). The non-linearity of these mixing curves was in good agreement with cooperative formation of **12**<sup>4</sup> (**12**<sup>6</sup>); Hill plots of the above data fully

corroborated the presence of positive cooperativity ( $n_H = 2.0$ , not shown).<sup>[26]</sup>

The dependence of the CD spectrum of **12**<sup>4</sup> (**12**<sup>6</sup>) on ionic strength and pH evidenced the importance of constructive ionic interactions, that is, the interaction of Glu and Lys residues (Figure 5b and c). The only conceivable rationalization of these findings was the formation of rigid-rod  $\beta$ -barrels by multiple tripeptide interdigitation. Relatively minor changes of the CD spectrum of **12**<sup>4</sup> (**12**<sup>6</sup>) at pH < 3.5 and > 10.5 and at salt concentrations of up to 1 M, as well as stability toward heat (up to 65 °C, not shown) and dilution (nM concentrations, not shown), evidenced the robust supramolecular architecture of rigid-rod  $\beta$ -barrels **12**<sup>4</sup> (**12**<sup>6</sup>).

Interestingly, oligomer **12**<sup>n</sup> ( $n \approx 26$ , Figure 3d) exhibited a blue-shift for the <sup>1</sup>L absorptions (278 nm) and the corresponding first CD Cotton effect (288 nm, not shown). These hypsochromic effects were indicative for intermolecular  $\pi$ – $\pi$  interactions between oligophenylenic arene arrays.<sup>[12a–c]</sup> The underlying, evidently more complex, suprastructure was not further investigated.

In summary, the spectroscopic properties of rigid-rod  $\beta$ -barrels **12**<sup>4</sup> (**12**<sup>6</sup>), but not those of oligomer **12**<sup>n</sup>, were in good agreement with the molecular models (Figure 2) with respect to molecular weight (Figure 3a), stoichiometry (Figure 5a), and extratoroidal interaction of complementary Lys and Glu residues (Figure 5b and c). However, these results contained no information on the presence and properties of a hydrophobic interior. The capacity of rigid-rod  $\beta$ -barrels to encapsulate carotenoids of different length and hydrophobicity was therefore explored.

**Carotenoid encapsulation by rigid-rod  $\beta$ -barrels:** Molecular models of rigid-rod lipocalin **12**<sup>4</sup> revealed an intratoroidal, hydrophobic space that is roughly complementary to the rod-shape of a single carotenoid, while hexamer **12**<sup>6</sup> and higher oligomers appeared as “bicycle tires” that might possibly surround disc micellar carotenoids (Figure 2). These two possibilities for guest encapsulation were studied with the hydrophobic  $\beta$ -carotene **11**, the truncated  $\beta$ -apo-carotenal **18**, and the bolaamphiphilic,<sup>[27]</sup> biologically relevant zeaxanthin **9** and astaxanthin **10** (Table 1).

For encapsulation, carotenoids were solubilized in cholate micelles at pH 6.4. Mixed carotenoid/cholate micelles in hexane have blue-shifted absorption maxima between 436 and 450 nm (Table 1). Dialytic cholate removal resulted in complete precipitation for  $\beta$ -carotene (Table 1, entry 2), the formation of well-known H-aggregates for zeaxanthin (Table 1, entry 8),<sup>[18]</sup> and presumably unprecedented J-aggregates for astaxanthin (Table 1, entry 11). The presence of polyanion **14** during dialytic cholate removal did not change these outcomes significantly (Table 1, entries 3, 7, and 10). The presence of both polyanion **14** and the complementary polycation **13** inhibited aggregation of  $\beta$ -apo-carotenal (Table 1, entry 4) and zeaxanthin (Table 1, entry 6), inhibited precipitation of  $\beta$ -carotene (Table 1, entry 1), and had apparently little influence on the J-aggregation of astaxanthin (Table 1, entry 11). These last two effects were studied in more detail.

**Rigid-rod carotenolipocalin 19:** Spectroscopic studies of  $\beta$ -carotene solubilized in detergent-free water (Table 1, entry 1) were consistent with encapsulation of one polyene by tetramer **12**<sup>4</sup> to give rigid-rod carotenolipocalin **19** (Figure 6).

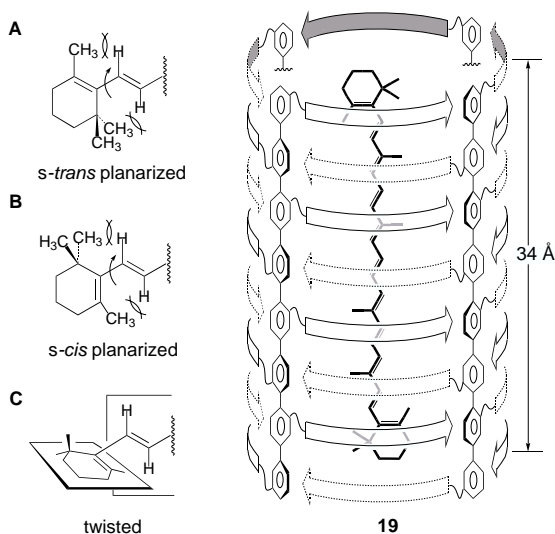


Figure 6. Rigid-rod carotenolipocalin **19**. Possible conformations with respect to the torsion angle between the polyene chain and the  $\beta$ -ionylidene ring of  $\beta$ -carotene **11** are shown on the left: *s-trans* (A) and *s-cis* planarized (B) conformers with maximal and twisted conformer (C) with minimal conjugation and nonbonded repulsion between  $\beta$ -ionylidene methyls and polyene hydrogens.

$\beta$ -Carotene encapsulation was distinguishable from simple binding by the absence of detectable interactions with preformed tetramer **12**<sup>4</sup> and, most importantly, the failure to extract  $\beta$ -carotene from capsule **19** into hexane.<sup>[28, 9b]</sup> It was, however, possible to deconstruct supramolecule **19** in THF. The relative chromophore absorption and fluorescence intensities in THF and water were consistent with an oligo(*p*-phenylene) to  $\beta$ -carotene ratio of  $\approx 4:1$ .

Rigid-rod carotenolipocalin **19** passed through Sephadex columns as a single band together with the oligo(*p*-phenylene) peptides. Size exclusion chromatography (SEC) revealed tetramers **12**<sup>4</sup> with traces of hexamers **12**<sup>6</sup> and oligomers **12**<sup>*n*</sup> (Figure 3e). Suppression of hexameric  $\beta$ -barrels **12**<sup>6</sup> suggested that  $\beta$ -carotene may act as hydrophobic template during the assembly of capsule **19**. The confirmed need of guest excess for successful assembly of **19** supported this role of  $\beta$ -carotene. An insufficient template effect could further explain why comparable host–guest complexes were not formed with the hydrophobically mismatched  $\beta$ -apo-carotenal **18** (Table 1, entry 4).

The interaction of oligo(*p*-phenylene) peptides and polyene in host–guest complex **19** was evidenced by CD spectroscopy and fluorescence quenching. On the one hand, the presence of monomeric  $\beta$ -carotene in a chiral environment was implied by induced CD (ICD) in the polyene region (Figure 7a). The slight offset of CD and absorption maxima (Figure 7b) of encapsulated  $\beta$ -carotene implied the additional presence of more complex and not yet understood effects. Oligo(*p*-phenylene)s with neighboring, energy-accepting  $\beta$ -carotene,

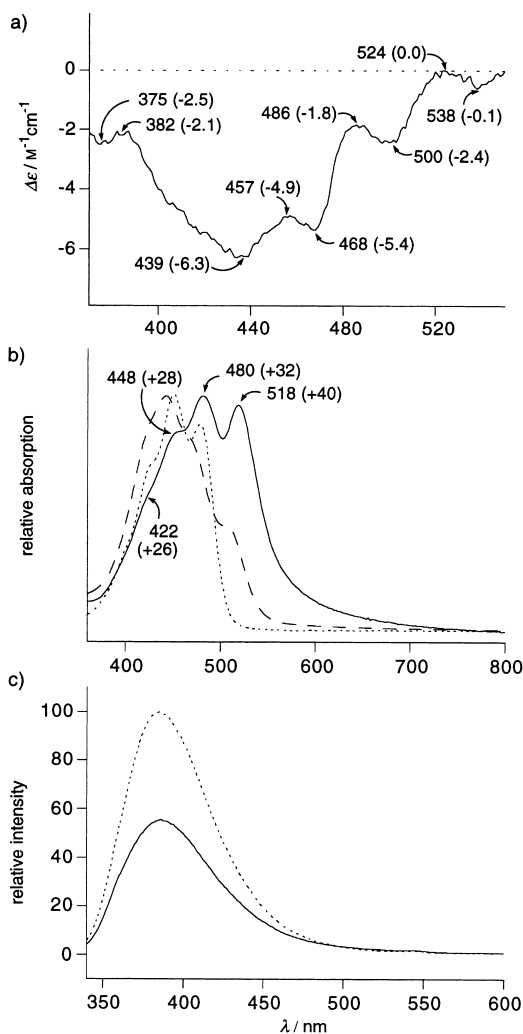


Figure 7. a) CD, b) UV/Vis, and c) fluorescence emission spectra of rigid-rod carotenolipocalin **19** in detergent-free water at pH 6.4. b) The normalized absorption spectrum of capsule **19** (solid line) in comparison to those of  $\beta$ -carotene **11** in cholate micelles (pH 6.4, dashed line) and in hexane (dotted line). The red shift of the maxima of **19** relative to that of **11** in hexane was determined using 2nd derivative spectra (not shown) and is given in parenthesis. c) Fluorescence emission spectrum of capsule **19** (solid line) in comparison to that of rigid-rod  $\beta$ -barrel **12**<sup>4</sup> (**12**<sup>6</sup>) (dotted line) at pH 6.4 (excitation: 316 nm). Both samples had identical emission intensity in THF.

on the other hand, were indicated by quenching of their fluorescence emission (Figure 7c). Note that 48% quenching is remarkable considering the short lifetime of the excited state of oligo(*p*-phenylene)s.<sup>[12f]</sup>

The absorption spectrum of lipocalin model **19** contained information on the nature of the intratoroidal space of rigid-rod  $\beta$ -barrel **12**<sup>4</sup> as expected. Namely, the  $\beta$ -carotene  $S_0 \rightarrow S_2$  transition in capsule **19** (Figure 7b, solid spectrum) was up to 40 nm red-shifted relative to that of  $\beta$ -carotene in hexane (Figure 7b, dotted spectrum), and its fine structure was well resolved. The symmetry-forbidden low-energy  $S_0 \rightarrow S_1$  transition was not observed.<sup>[14–16]</sup>

These spectroscopic features indicate that  $\beta$ -carotene is a) in hydrophobic environment (no blue shift)<sup>[13]</sup> and b) monomeric (no broadening).<sup>[14]</sup> To explain the observed bathochromic effect, consideration of solvent polarity is clearly not suffi-

cient; it further indicates extension of  $\beta$ -carotene conjugation by ring–chain co-planarization (Figure 6A and B). This implies that the polyene chromophore with twisted conformation in solution is flattened by rigid-rod  $\beta$ -barrel **12**<sup>4</sup> to fit the internal hydrophobic channel in capsule **19**. Very similar changes in the absorption spectrum of retinol upon binding to lipocalin  $\beta$ -lactoglobulin have been explained by ring–chain co-planarization.<sup>[9]</sup> Moreover, the observed red shift and increase in fine structure for encapsulated  $\beta$ -carotene are in excellent agreement with theoretical models for carotenoid planarization.<sup>[17]</sup>

In summary, we have shown that monomeric  $\beta$ -carotene can be encapsulated by rigid-rod lipocalin **12**<sup>4</sup> to quantitatively yield host–guest complex **19** in detergent-free water. The usefulness of  $\beta$ -carotene as probe for the hydrophobic interior of rigid-rod  $\beta$ -barrel **12**<sup>4</sup> was evidenced by a remarkable bathochromic effect (presumably) due to planarization of the polyene within the complementary “innermolecular”<sup>[28]</sup> space.

**Mixed rigid-rod disc micelles 20:** The influence of complementary oligo(*p*-phenylene) peptides **13** and **14** on formation of astaxanthin J-aggregates by dialytic detergent removal seemed initially negligible. A remarkable red shift of  $\approx 90$  nm with respect to astaxanthin absorption in hexane was observed with and without rods (Table 1, entries 9–11). Indications for the formation of mixed disc micelles **20** (Figure 8)

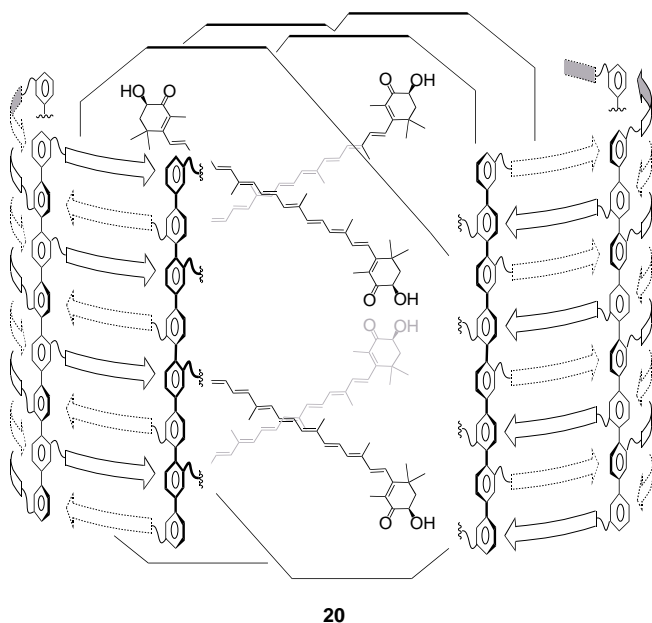


Figure 8. Tentative structure of astaxanthin/oligo(*p*-phenylene) disc micelles **20**.

were found by CD spectroscopy (Figure 9). Strong bisignate CD Cotton effects ( $A = -110$ ) centered around the red-shifted astaxanthin absorption evidenced exciton coupling that was consistent with carotenoid aggregation. The presence of complementary oligo(*p*-phenylene) peptides during dialytic detergent removal caused inversion of the absolute sense

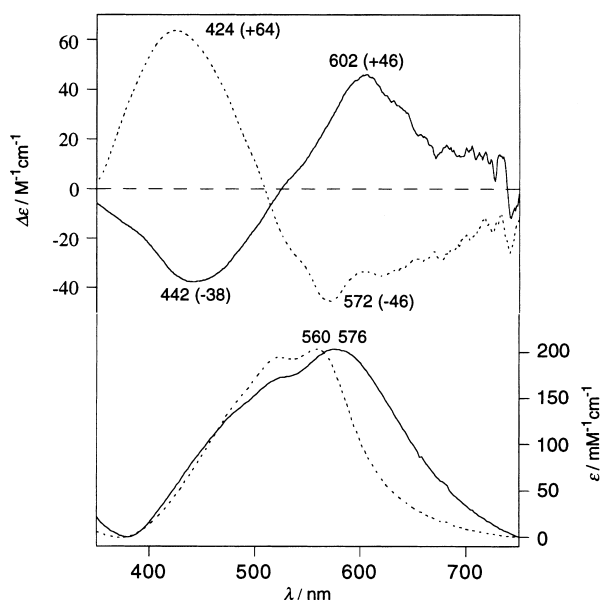


Figure 9. Absorption (bottom) and CD (top) spectra of astaxanthin aggregates at pH 6.4 prepared in the presence (solid lines) and absence (dotted lines) of octi(*p*-phenylene)s **13** and **14**.

of twist of these astaxanthin aggregates ( $A = +84$ ). Control experiments corroborated that addition of rigid-rod  $\beta$ -barrels **12**<sup>4</sup> (**12**<sup>6</sup>) to preformed astaxanthin aggregates ( $A = -110$ ) and dialysis with polyanionic rod **14** only do not yield astaxanthin aggregates with positive amplitude. These findings were consistent with the formation of mixed-disc micelles **20** during dialytic detergent removal.

The quenching efficiency of astaxanthin in disc micelles **20** is 50% of that of  $\beta$ -carotene in rigid-rod carotenolipocalin **19** (Table 1, entries 9 and 1). Gel filtration of supramolecule **20** yielded a single product that contained both oligo(*p*-phenylene)s and astaxanthin, while astaxanthin J-aggregates without both rods were retained on Sephadex columns due to dilution below critical aggregation concentration (Table 1, entries 9–11). SEC with disc micelles **20** gave not reproducible results. However, an occasionally observed broad peak with MW  $\approx 84000$  and the spectroscopically estimated 1:1 stoichiometry suggests that disc micelles **20** may consist of dodecameric rigid-rod  $\beta$ -barrels surrounding twelve J-aggregated astaxanthin molecules (Figure 8). Similar “bicycle tire” structures have been observed before with amphiphilic proteins (e.g., apolipoproteins), peptides (e.g., melittin), and detergents (e.g., lysophosphatidylcholine).<sup>[29]</sup>

The capacity of rigid-rod  $\beta$ -barrels to stabilize small J-aggregates is of high interest with respect to the significance of J-aggregates in biological pigmentation in general<sup>[30]</sup> and that of marine invertebrates in particular.<sup>[8]</sup> As mentioned in the introduction, the blue color of the lobster *Humarus gammarus* may originate from binding of two astaxanthins ( $\lambda_{\max} \approx 472$  nm) to  $\beta$ -crustacyanidin dimers ( $\lambda_{\max} \approx 585$  nm,  $A \approx -30$ ) followed by aggregation into  $\alpha$ -crustacyanidin ( $\lambda_{\max} \approx 630$  nm,  $A \approx -95$ ).<sup>[8]</sup> Here we have shown that astaxanthin J-aggregates with similar spectroscopic properties ( $\lambda_{\max} \approx 560$  nm,  $A \approx -110$ ) can be prepared by dialytic detergent removal, and that their structure, stability and stereo-



chemistry can be controlled by surrounding rigid-rod  $\beta$ -barrels ( $\lambda_{\max} \approx 576$  nm,  $A \approx +84$ ). These findings may thus contribute to the understanding of the molecular mechanisms of invertebrate coloration.

## Conclusion

With the present study, we demonstrate the capacity of complementary oligo(*p*-phenylene) peptides to form water-soluble, expanded rigid-rod  $\beta$ -barrels with defined length, flexible diameter, and lipocalin-type toroidal amphiphilicity. Spectroscopic evidence was obtained for the designed role of multiple extratoroidal electrostatic and intratoroidal hydrophobic interactions. Encapsulation of hydrophobic guests by rigid-rod  $\beta$ -barrels was shown to depend on hydrophobic matching and guest polarity. Both tetrameric rigid-rod carotenolipocalins with one encapsulated hydrophobic guest and more fragile rigid-rod disc micelles with J-aggregated bolaamphiphiles were observed.

These results suggest that rigid-rod  $\beta$ -barrels may serve as general models for biological  $\beta$ -barrels; this implies an extremely diverse potential applicability of these unique toroidal supramolecules for biomimetic pigmentation,<sup>[6–8, 30]</sup> membrane-protein solubilization,<sup>[1, 5]</sup> gene transfection,<sup>[3, 5]</sup> and catalysis in the broadest sense.<sup>[2, 4, 31]</sup> Studies along these lines are ongoing.

## Experimental Section

**General:** Reagents for synthesis were purchased from Aldrich. PyBOP was from Calbiochem-Novabiochem. Amino acid derivatives were obtained from Calbiochem-Novabiochem and Bachem. Zeaxanthin was from Indofine Chemical Company, astaxanthin from Alexis Biochemicals,  $\beta$ -apo-8'-carotenal from Fluka, and  $\beta$ -carotene from Aldrich. Sephadex G-50, sodium cholate and other salts were of the best grade available from Sigma Chemicals. Solvents were distilled and, if necessary, dried before use. All reactions were performed under nitrogen atmosphere. Column chromatography was carried out over silica gel (Selecto Scientific, 32–6  $\mu$ m). Analytical thin-layer chromatography (TLC) was performed on AL SIL G/UV (Whatman). Preparative TLC (PTLC) was performed on silica gel 60F-254 (Merck) or silica gel GF-2 (Aldrich). The values of optical rotation  $[\alpha]_D^{20}$  were determined at room temperature on a Perkin–Elmer 241 Polarimeter and are given in degrees. Melting points (mp) were determined on a heating table from Reichert (Austria). IR-spectra were recorded in KBr pellets on a Perkin–Elmer FT-IR Spectrometer Paragon 500 and are reported in  $\text{cm}^{-1}$  (intensity: w = weak, m = medium, s = strong).  $^1\text{H}$  NMR spectra were recorded on a Varian Mercury 300 spectrometer, a Bruker AMX 400 spectrometer, and a Varian UNITY INOVA 500 MHz spectrometer. Chemical shifts are reported in ppm relative to TMS ( $\delta = 0$ ). Spin multiplicities are reported as singlet (s), doublet (d), triplet (t), quartet (q) or multiplet (m), and coupling constants ( $J$ ) are given in Hz.  $^1\text{H}$  NMR resonances were assigned with the aid of additional information from pertinent 2D NMR spectra (H, H-COSY, NOESY, ROESY, and TOCSY). The presence of solvent in analytical samples was corroborated by  $^1\text{H}$  NMR spectroscopy. FAB-HRMS was performed on a Fenningan 3200 twin-quadrupole mass spectrometer at the University of Maryland, College Park. ESI-MS was performed on a PE-Sciex API 100 electrospray instrument by the Lombardi Cancer Center's Macromolecular Analysis Shared Resource. MALDI-TOF-MS was performed on a Proflex Bruker mass spectrometer at the University of Maryland, College Park, using a DHB (2,5 dihydroxy benzoic acid) matrix. Dialysis was performed with a Mini Lipoprep® (Sialomed) or dialysis cells from Fisher Scientific with dialysis membranes from Diachema (MW-cutoff = 5000). Gel filtration (GF) was

performed over Sephadex G-50 (1  $\times$  27 cm). Size-exclusion chromatography (SEC) was performed on Superdex® 75 HR 10/30 prepacked column from Pharmacia Biotech (MW 70000–3000, 1 mL buffer per min) coupled with a Jasco PU-980 pump and a Jasco UV-970 UV-Vis detector. MWs were determined by using the protein standards albumin (67.0 kDa), ovalbumin (43.0 kDa), chymotrypsinogen A (25.0 kDa), ribonuclease A (13.7 kDa), and aprotinin (6.5 kDa) from Pharmacia Biotech. Fluorescence spectra were recorded on FluoroMax-2 (Jobin Yvon-Spex). Both emission and excitation spectra were not corrected. CD-spectra were recorded on JASCO-710 and JASCO-715 spectropolarimeters and reported as  $\Delta\epsilon_{\max}$  [ $\text{M}^{-1}\text{cm}^{-1}$ ] at  $\lambda_{\max}$  [nm]. UV-Vis spectra were recorded on a Hewlett–Packard 8452A diode array spectrophotometer or on a Varian Cary 1 Bio spectrophotometer and are reported as  $\lambda_{\max}$  [nm] ( $\epsilon_{\max}$  [ $\text{mM}^{-1}\text{cm}^{-1}$ ]).

**Z-Leu-Lys(Boc)-NH<sub>2</sub> (general procedure A):** 1-(3-Dimethylaminopropyl)-3-ethyl-carbodiimide·HCl (288 mg, 1.5 mmol), 1-hydroxybenzotriazole (172 mg, 1.27 mmol), Z-Leu-OH (282 mg, 1.06 mmol) and triethylamine (0.441 mL, 6 mmol) were added to a solution of H-Lys(Boc)-NH<sub>2</sub>·HCl (300 mg, 1.06 mmol) in  $\text{CH}_2\text{Cl}_2$  (5.31 mL) at 0 °C. After stirring for 6 h in the dark at RT, the reaction mixture was diluted with  $\text{CH}_2\text{Cl}_2$ , extracted with saturated aqueous  $\text{NaHCO}_3$ , washed with brine, extracted with 1M aqueous  $\text{KHSO}_4$ , washed with brine, dried over anhydrous  $\text{Na}_2\text{SO}_4$ , and concentrated in vacuo. Purification of the crude product by column chromatography ( $\text{CH}_2\text{Cl}_2/\text{MeOH}$  10:1,  $R_f = 0.4$ ) yielded pure Z-Leu-Lys(Boc)-NH<sub>2</sub> (489 mg, 93 %) as a white powder.  $[\alpha]_D^{20} = -15.8$  ( $c = 1.00$  in MeOH); m.p. 165.1–167.0 °C; IR (KBr):  $\tilde{\nu} = 3392$  (s), 3374 (s), 3215 (m), 3070 (w), 3039 (w), 2956 (m), 2935 (m), 2867 (w), 1685 (s), 1643 (s), 1534 (s), 1452 (m), 1420 (w), 1390 (w), 1363 (m), 1275 (s), 1254 (s), 1171 (s), 1124 (w), 1052 (w), 912 (w), 865 (w), 782 (w), 735 (w), 694 (m), 647  $\text{cm}^{-1}$  (w);  $^1\text{H}$  NMR (300 MHz,  $[\text{D}]_6\text{DMSO}$ , 25 °C, TMS):  $\delta = 7.80$ –7.73 (m, 1H; Lys-NH, exchange with  $\text{D}_2\text{O}$ ), 7.52–7.43 (m, 1H; Leu-NH, exchange with  $\text{D}_2\text{O}$ ), 7.34–7.29 (m, 6H; ArH and Lys-CONH<sub>2</sub>, partial exchange with  $\text{D}_2\text{O}$ ), 7.04–6.97 (m, 1H; Lys-CONH<sub>2</sub>, exchange with  $\text{D}_2\text{O}$ ), 6.78–6.71 (m, 1H; Boc-NH, exchange with  $\text{D}_2\text{O}$ ), 5.04–5.00 (m, 2H; ArCH<sub>2</sub>), 4.20–4.12 (m, 1H; Lys-H <sub>$\alpha$</sub> ), 4.06–3.96 (m, 1H; Leu-H <sub>$\alpha$</sub> ), 2.96–2.78 (m, 2H; Lys-H <sub>$\beta$</sub> ), 1.70–1.20 (several m, 9H; Leu-H <sub>$\beta,\gamma$</sub> , Lys-H <sub>$\beta,\gamma,\delta$</sub> ), 1.35 (s, 9H; Boc-CH<sub>3</sub>), 0.90–0.80 (m, 6H; Leu-CH<sub>3</sub>).

**H-Leu-Lys(Boc)-NH<sub>2</sub> (general procedure B):** A catalytic amount of Pd/C was added to a solution of Z-Leu-Lys(Boc)-NH<sub>2</sub> (498 mg, 1.01 mmol) in MeOH (5 mL). The suspension was degassed at least four times and set under an H<sub>2</sub> atmosphere. After stirring for 2 h, the Pd/C was filtered off and the crude product was concentrated in vacuo. Column chromatography ( $\text{CH}_2\text{Cl}_2/\text{MeOH}/i\text{Pr-NH}_2$  90:9:1,  $R_f = 0.4$ ) yielded pure H-Leu-Lys(Boc)-NH<sub>2</sub> as a white powder (284 mg, 0.79 mmol, 80 %).  $[\alpha]_D^{20} = -0.4$  ( $c = 1.00$  in MeOH); m.p. 109.3–110.8 °C; IR (KBr):  $\tilde{\nu} = 3352$  (s), 3325 (s), 3200 (w), 2933 (m), 2868 (w), 1688 (s), 1669 (s), 1615 (s), 1536 (s), 1465 (w), 1441 (w), 1389 (w), 1367 (m), 1283 (m), 1250 (m), 1180 (m), 1123 (w), 1006 (w), 659 (w), 588  $\text{cm}^{-1}$  (w);  $^1\text{H}$  NMR (300 MHz,  $[\text{D}]_6\text{DMSO}$ , 25 °C, TMS):  $\delta = 8.03$ –7.87 (m, 1H; Lys-NH, exchange with  $\text{D}_2\text{O}$ ), 7.50–7.30 (m, 1H; Lys-CONH<sub>2</sub>, exchange with  $\text{D}_2\text{O}$ ), 7.10–6.98 (m, 1H; Lys-CONH<sub>2</sub>, exchange with  $\text{D}_2\text{O}$ ), 6.76–6.72 (m, 1H; Boc-NH, exchange with  $\text{D}_2\text{O}$ ), 4.18–4.10 (m, 1H; Lys-H <sub>$\alpha$</sub> ), 3.22–3.15 (m, 1H; Leu-H <sub>$\alpha$</sub> ), 2.90–2.81 (m, 2H; Lys-H <sub>$\beta$</sub> ), 1.80–1.10 (several m, 9H; Leu-H <sub>$\beta,\gamma$</sub> , Lys-H <sub>$\beta,\gamma,\delta$</sub> ), 1.35 (s, 9 Boc-CH<sub>3</sub>), 0.87 (d,  $^3J(\text{H,H}) = 6.6$  Hz, 3H; Leu-CH<sub>3</sub>), 0.83 (d,  $^3J(\text{H,H}) = 6.6$  Hz, 3H; Leu-CH<sub>3</sub>).

**Z-Lys(Boc)-Leu-Lys(Boc)-NH<sub>2</sub>:** Coupling of H-Leu-Lys(Boc)-NH<sub>2</sub> (284 mg, 0.79 mmol) and Z-Lys(Boc)-OH (452 mg, 1.19 mmol) by following procedure A and purification of the crude product by column chromatography ( $\text{CH}_2\text{Cl}_2/\text{MeOH}$  10:1,  $R_f = 0.3$ ) yielded pure Z-Lys(Boc)-Leu-Lys(Boc)-NH<sub>2</sub> (464 mg, 82 %) as a white powder.  $[\alpha]_D^{20} = -23.0$  ( $c = 1.00$  in MeOH); m.p. 177.5–178.9 °C; IR (KBr):  $\tilde{\nu} = 3314$  (s), 2934 (s), 2869 (m), 2373 (w), 1686 (s), 1635 (s), 1534 (s), 1458 (w), 1391 (w), 1367 (m), 1269 (m), 1252 (m), 1174 (m), 1057 (w), 868 (w), 778 (w), 754 (w), 699 (w), 641  $\text{cm}^{-1}$  (w);  $^1\text{H}$  NMR (300 MHz,  $[\text{D}]_6\text{DMSO}$ , 25 °C, TMS):  $\delta = 7.98$ –7.92 (m, 1H; Lys-NH, exchange with  $\text{D}_2\text{O}$ ), 7.73–7.66 (m, 1H; Leu-NH, exchange with  $\text{D}_2\text{O}$ ), 7.43–7.25 (several m, 6H; ArH and Lys-NH, partial exchange with  $\text{D}_2\text{O}$ ), 7.25–7.20 (m, 1H; Lys-CONH<sub>2</sub>, exchange with  $\text{D}_2\text{O}$ ), 7.03–6.97 (m, 1H; Lys-CONH<sub>2</sub>, exchange with  $\text{D}_2\text{O}$ ), 6.80–6.70 (m, 2H; Boc-NH), 5.00 (s, 2H; ArCH<sub>2</sub>), 4.32–4.20 (m, 1H; Lys-H <sub>$\alpha$</sub> ), 4.20–4.05 (m, 1H; Leu-H <sub>$\alpha$</sub> ), 4.02–3.88 (m, 1H; Lys-H <sub>$\alpha$</sub> ), 2.95–2.78 (m, 4H; Lys-H <sub>$\beta$</sub> ), 1.70–1.10 (several m, 15H; Leu-H <sub>$\beta,\gamma$</sub> , Lys-H <sub>$\beta,\gamma,\delta$</sub> ), 1.34 (s, 18H; Boc-CH<sub>3</sub>), 0.86 (d,  $^3J(\text{H,H}) = 6.6$  Hz, 3H; Leu-CH<sub>3</sub>), 0.81 (d,  $^3J(\text{H,H}) = 6.6$  Hz, 3H; Leu-CH<sub>3</sub>).



**H-Lys(Boc)-Leu-Lys(Boc)-NH<sub>2</sub>**: Deprotection of Z-Lys(Boc)-Leu-Lys(Boc)-NH<sub>2</sub> (464 mg, 0.64 mmol) by following procedure B and purification by column chromatography (CH<sub>2</sub>Cl<sub>2</sub>/MeOH/*i*Pr-NH<sub>2</sub> 90:9:1, *R<sub>f</sub>* = 0.4) yielded pure H-Lys(Boc)-Leu-Lys(Boc)-NH<sub>2</sub> as a white powder (328 mg, 87%). [ $\alpha$ ]<sub>D</sub><sup>20</sup> = -17.0 (*c* = 1.00 in MeOH); m.p. 76.0–77.2 °C; IR (KBr):  $\tilde{\nu}$  = 3342 (s), 3061 (w), 2937 (m), 2864 (w), 2356 (w), 1685 (s), 1529 (s), 1457 (w), 1394 (w), 1368 (m), 1275 (w), 1249 (m), 1171 (m), 1046 (w), 1010 (w), 865 (w), 782 (w), 652 cm<sup>-1</sup> (w); <sup>1</sup>H NMR (300 MHz, [D]<sub>6</sub>DMSO, 25 °C, TMS):  $\delta$  = 8.03–7.94 (m, 1H; Lys-NH, exchange with D<sub>2</sub>O), 7.85–7.78 (m, 1H; Leu-NH, exchange with D<sub>2</sub>O), 7.27–7.21 (m, 1H; Lys-CONH<sub>2</sub>, exchange with D<sub>2</sub>O), 7.00–6.93 (s, 1H; Lys-CONH<sub>2</sub>, exchange with D<sub>2</sub>O), 6.78–6.68 (m, 2H; Boc-NH, exchange with D<sub>2</sub>O), 4.37–4.22 (m, 1H; Lys-H <sub>$\alpha$</sub> ), 4.18–4.05 (m, 1H; Leu-H <sub>$\alpha$</sub> ), 3.20–3.08 (m, 1H; Lys-H <sub>$\alpha$</sub> ), 2.92–2.78 (m, 4H; Leu-H <sub>$\alpha$</sub> ), 1.70–1.10 (several m, 15H; Leu-H <sub>$\beta,\gamma,\delta$</sub> , Lys-H <sub>$\beta,\gamma,\delta$</sub> ), 1.36 (s, 18H; Boc-CH<sub>3</sub>), 0.86 (d, <sup>3</sup>*J*(H,H) = 6.6 Hz, 3H; Leu-CH<sub>3</sub>), 0.81 (d, <sup>3</sup>*J*(H,H) = 6.6 Hz, 3H; Leu-CH<sub>3</sub>); HRMS (FAB): *m/z* calcd for C<sub>28</sub>H<sub>54</sub>N<sub>6</sub>O<sub>7</sub>; 587.41321; found 587.41586.

**Z-Leu-Glu(OtBu)-NH<sub>2</sub>**: Coupling of H-Glu(OtBu)-NH<sub>2</sub>·HCl (240 mg, 1.25 mmol) and Z-Leu-OH (331 mg, 1.25 mmol) by following procedure A and purification of the crude product by column chromatography (CH<sub>2</sub>Cl<sub>2</sub>/MeOH 20:1, *R<sub>f</sub>* = 0.3) yielded pure Z-Leu-Glu(OtBu)-NH<sub>2</sub> (474 mg, 84%) as a white powder. [ $\alpha$ ]<sub>D</sub><sup>20</sup> = -22.0 (*c* = 1.00 in MeOH); m.p. 140.6–141.2 °C; IR (KBr):  $\tilde{\nu}$  = 3388 (s), 3316 (s), 3209 (m), 3068 (w), 3036 (w), 2959 (m), 2933 (m), 2874 (w), 1730 (s), 1674 (s), 1644 (s), 1531 (s), 1468 (w), 1455 (w), 1420 (w), 1393 (w), 1368 (m), 1287 (m), 1261 (m), 1236 (m), 1159 (m), 1123 (w), 1051 (w), 993 (w), 958 (w), 913 (w), 849 (w), 780 (w), 744 (w), 696 (m), 645 cm<sup>-1</sup> (w); <sup>1</sup>H NMR (300 MHz, [D]<sub>6</sub>DMSO, 25 °C, TMS):  $\delta$  = 7.85 (d, <sup>3</sup>*J*(H,H) = 8.0 Hz, 1H; Glu-NH, exchange with D<sub>2</sub>O), 7.48 (d, <sup>3</sup>*J*(H,H) = 8.2 Hz, 1H; Leu-NH, exchange with D<sub>2</sub>O), 7.38–7.24 (m, 6H; , ArH and Glu-CONH<sub>2</sub>, partial exchange with D<sub>2</sub>O), 7.10–7.04 (m, 1H; Glu-CONH<sub>2</sub>, exchange with D<sub>2</sub>O), 5.01 (s, 2H; ArCH<sub>2</sub>), 4.24–4.13 (m, 1H; Glu-H <sub>$\alpha$</sub> ), 4.07–3.96 (m, 1H; Leu-H <sub>$\alpha$</sub> ), 2.23–2.12 (m, 2H; Glu-H <sub>$\alpha$</sub> ), 1.96–1.33 (m, 5H; Glu-H <sub>$\beta$</sub>  and Leu-H <sub>$\beta$</sub> ), 1.37 (s, 9H; *t*Bu), 0.90–0.79 (m, 6H; Leu-CH<sub>3</sub>).

**H-Leu-Glu(OtBu)-NH<sub>2</sub>**: Deprotection of Z-Leu-Glu(OtBu)-NH<sub>2</sub> (474 mg, 1.05 mmol) by following procedure B and purification by column chromatography (CH<sub>2</sub>Cl<sub>2</sub>/MeOH/*i*Pr-NH<sub>2</sub> 90:9:1, *R<sub>f</sub>* = 0.3) yielded pure H-Leu-Glu(OtBu)-NH<sub>2</sub> (274 mg, 83%) as a colorless gum. [ $\alpha$ ]<sub>D</sub><sup>20</sup> = -2.2 (*c* = 1.00 in MeOH); IR (KBr):  $\tilde{\nu}$  = 3345 (s), 3202 (m), 2953 (s), 2868 (m), 1726 (s), 1660 (s), 1517 (m), 1468 (w), 1454 (w), 1419 (w), 1392 (w), 1369 (m), 1321 (w), 1290 (w), 1255 (m), 1157 (s), 1034 (w), 957 (w), 920 (w), 846 (w), 753 (w), 650 cm<sup>-1</sup> (w); <sup>1</sup>H NMR (300 MHz, [D]<sub>6</sub>DMSO, 25 °C, TMS):  $\delta$  = 8.04–7.91 (m, 2H; Glu-NH, Leu-NH, exchange with D<sub>2</sub>O), 7.42–7.33 (m, 1H; Glu-CONH<sub>2</sub>, exchange with D<sub>2</sub>O), 7.14–7.04 (m, 1H; Glu-CONH<sub>2</sub>, exchange with D<sub>2</sub>O), 4.25–4.14 (m, 1H; Glu-H <sub>$\alpha$</sub> ), 3.20–3.12 (m, 1H; Leu-H <sub>$\alpha$</sub> ), 2.22–2.09 (m, 2H; Glu-H <sub>$\alpha$</sub> ), 1.98–1.60 (m, 5H; Glu-H <sub>$\beta$</sub> , Leu-H <sub>$\beta,\gamma$</sub> ), 1.37 (s, 9H; *t*Bu), 0.86 (d, <sup>3</sup>*J*(H,H) = 6.6 Hz, 3H; Leu-CH<sub>3</sub>), 0.83 (d, <sup>3</sup>*J*(H,H) = 6.6 Hz, 3H; Leu-CH<sub>3</sub>).

**Z-Glu(OtBu)-Leu-Glu(OtBu)-NH<sub>2</sub>**: Coupling of H-Leu-Glu(OtBu)-NH<sub>2</sub> (274 mg, 0.87 mmol) and Z-Glu(OtBu)-OH (440 mg, 1.31 mmol) by following procedure A and purification of the crude product by column chromatography (CH<sub>2</sub>Cl<sub>2</sub>/MeOH 20:1, *R<sub>f</sub>* = 0.25) yielded pure Z-Glu(OtBu)-Leu-Glu(OtBu)-NH<sub>2</sub> (486 mg, 88%) as a white powder. [ $\alpha$ ]<sub>D</sub><sup>20</sup> = -29.0 (*c* = 1.00 in MeOH); m.p. 172.8–174.2 °C; IR (KBr):  $\tilde{\nu}$  = 3307 (s), 3067 (w), 2978 (m), 2934 (m), 1731 (s), 1670 (s), 1637 (s), 1534 (s), 1454 (m), 1393 (m), 1368 (s), 1256 (s), 1156 (s), 1054 (w), 953 (w), 850 (w), 753 (w), 698 cm<sup>-1</sup> (m); <sup>1</sup>H NMR (300 MHz, [D]<sub>6</sub>DMSO, 25 °C, TMS):  $\delta$  = 7.96 (d, <sup>3</sup>*J*(H,H) = 8.0 Hz, 1H; Glu-NH, exchange with D<sub>2</sub>O), 7.85 (d, <sup>3</sup>*J*(H,H) = 8.0 Hz, 1H; Glu-NH, exchange with D<sub>2</sub>O), 7.46 (d, <sup>3</sup>*J*(H,H) = 8.2 Hz, 1H; Leu-NH, exchange with D<sub>2</sub>O), 7.34 (m, 5H; ArH), 7.24–7.18 (m, 1H; Lys-CONH<sub>2</sub>, exchange with D<sub>2</sub>O), 7.08–7.00 (m, 1H; Lys-CONH<sub>2</sub>, exchange with D<sub>2</sub>O), 5.06–4.95 (m, 2H; ArCH<sub>2</sub>), 4.34–4.22 (m, 1H; Glu-H <sub>$\alpha$</sub> ), 4.23–4.09 (m, 1H; Leu-H <sub>$\alpha$</sub> ), 4.05–4.09 (m, 1H; Glu-H <sub>$\alpha$</sub> ), 2.29–2.12 (m, 4H; Lys-H <sub>$\alpha$</sub> ), 1.96–1.20 (m, 7H; Leu-H <sub>$\beta,\gamma$</sub> , Glu-H <sub>$\beta$</sub> ), 1.37 (s, 18H; *t*Bu), 0.87 (d, <sup>3</sup>*J*(H,H) = 6.6 Hz, 3H; Leu-CH<sub>3</sub>), 0.81 (d, <sup>3</sup>*J*(H,H) = 6.6 Hz, 3H; Leu-CH<sub>3</sub>).

**H-Glu(OtBu)-Leu-Glu(OtBu)-NH<sub>2</sub>**: Deprotection of Z-Glu(OtBu)-Leu-Glu(OtBu)-NH<sub>2</sub> (486 mg, 0.77 mmol) by following procedure B and purification by column chromatography (CH<sub>2</sub>Cl<sub>2</sub>/MeOH/*i*Pr-NH<sub>2</sub> 90:9:1, *R<sub>f</sub>* = 0.4) yielded pure H-Glu(OtBu)-Leu-Glu(OtBu)-NH<sub>2</sub> (358 mg, 93%) as a white powder. [ $\alpha$ ]<sub>D</sub><sup>20</sup> = -38.5 (*c* = 1.00 in MeOH); m.p. 85.5–86.2 °C; IR (KBr):  $\tilde{\nu}$  = 3306 (s), 3070 (w), 2977 (m), 2934 (m), 2870 (w), 2354 (w), 1729 (s), 1650 (s), 1542 (m), 1453 (w), 1368 (s), 1257 (m), 1156 (s), 956 (w), 849

(w), 666 cm<sup>-1</sup> (w); <sup>1</sup>H NMR (300 MHz, [D]<sub>6</sub>DMSO, 25 °C, TMS):  $\delta$  = 8.04–7.89 (m, 2H; Glu-NH, Leu-NH, exchange with D<sub>2</sub>O), 7.28–7.20 (s, 1H; Glu-CONH<sub>2</sub>, exchange with D<sub>2</sub>O), 7.08–7.00 (s, 1H; Glu-CONH<sub>2</sub>, exchange with D<sub>2</sub>O), 4.34–4.22 (m, 1H; Glu-H <sub>$\alpha$</sub> ), 4.20–4.09 (m, 1H; Leu-H <sub>$\alpha$</sub> ), 3.19–3.08 (m, 1H; Glu-H <sub>$\alpha$</sub> ), 2.29–2.12 (m, 4H; Glu-H <sub>$\beta$</sub> ), 2.00–1.30 (m, 9H; Leu-H <sub>$\beta,\gamma$</sub> , Glu-H <sub>$\beta$</sub> ), 1.37 (s, 18H; *t*Bu), 0.87 (d, <sup>3</sup>*J*(H,H) = 6.6 Hz, 3H; Leu-CH<sub>3</sub>), 0.84 (d, <sup>3</sup>*J*(H,H) = 6.6 Hz, 3H; Leu-CH<sub>3</sub>); HRMS (FAB): *m/z* calcd for C<sub>24</sub>H<sub>44</sub>N<sub>4</sub>O<sub>7</sub>; 501.32883; found 501.32838.

**8<sup>3</sup>,7<sup>2</sup>,6<sup>3</sup>,5<sup>2</sup>,4<sup>3</sup>,3<sup>2</sup>,2<sup>3</sup>,1<sup>3</sup>-Octa(hydroxycarbonylmethoxy)-*p*-octiphenyl (15) (general procedure C)**: TFA (1 mL) was added to a solution of 8<sup>3</sup>,7<sup>2</sup>,6<sup>3</sup>,5<sup>2</sup>,4<sup>3</sup>,3<sup>2</sup>,2<sup>3</sup>,1<sup>3</sup>-octa(*tert*-butoxycarbonylmethoxy)-*p*-octiphenyl<sup>[10, 12a-g]</sup> (6.8 mg, 4.2  $\mu$ mol) in CH<sub>2</sub>Cl<sub>2</sub> (1 mL). After stirring for 45 min at RT, the reaction mixture was concentrated in vacuo to give pure **15** (5.0 mg, 100%) as a white solid. <sup>1</sup>H NMR (300 MHz, CDCl<sub>3</sub>/CD<sub>3</sub>OD 1:1, 25 °C, TMS):  $\delta$  = 7.48–7.41 (m, 6H; ArH), 7.37–7.37–7.12 (m, 16H; ArH), 6.91 (dd, <sup>3</sup>*J*(H,H) = 5.8 Hz, <sup>4</sup>*J*(H,H) = 2.2 Hz, 2H; ArH), 4.69 (s, 16H; ArOCH<sub>2</sub>); MS (MALDI-TOF): *m/z* calcd for C<sub>64</sub>H<sub>50</sub>O<sub>24</sub>; 1203.08; found 1203.66.

**8<sup>3</sup>,7<sup>2</sup>,6<sup>3</sup>,5<sup>2</sup>,4<sup>3</sup>,3<sup>2</sup>,2<sup>3</sup>,1<sup>3</sup>-Octa(NH<sub>2</sub>-Glu(OtBu)-Leu-Glu(OtBu)-carbonylmethoxy)-*p*-octiphenyl (17)**: Coupling of **15** (4.5 mg, 3.74  $\mu$ mol) in DMSO (1 mL, instead of CH<sub>2</sub>Cl<sub>2</sub>) and H-Glu(OtBu)-Leu-Glu(OtBu)-NH<sub>2</sub> (45 mg, 89  $\mu$ mol) by following procedure A, and purification of the crude product by PTLC (CH<sub>2</sub>Cl<sub>2</sub>/MeOH/toluene 10:1:1, *R<sub>f</sub>* = 0.1, and CH<sub>2</sub>Cl<sub>2</sub>/MeOH 10:1, *R<sub>f</sub>* = 0.5) yielded pure **17** (12.9 mg, 67%) as a white solid. <sup>1</sup>H NMR (500 MHz, CDCl<sub>3</sub>/CD<sub>3</sub>OD 1:1, 25 °C, TMS):  $\delta$  = 7.58–7.24 (m, 24H; ArH), 6.98 (d, <sup>3</sup>*J*(H,H) = 7.7 Hz, 2H; ArH), 4.80–4.20 (several m, 40H; ArOCH<sub>2</sub>, Leu-H <sub>$\alpha$</sub> , Glu-H <sub>$\alpha$</sub> ), 2.40–2.20 (m, 32H; Glu-H <sub>$\alpha$</sub> ), 2.16–1.50 (several m, 56H; Leu-H <sub>$\beta,\gamma$</sub> , Glu-H <sub>$\beta$</sub> ), 1.41–1.29 (m, 144H; *t*Bu), 0.95–0.80 (m, 48H; Leu-CH<sub>3</sub>); MS (ESI, MeOH, 1% formic acid): *m/z* (%): 1289 (97) [*M*+Na]<sup>+</sup>, 1711 (100) [*M*+Na]<sup>2+</sup>, 2555 (20) [*M*+Na]<sup>2+</sup>.

**8<sup>3</sup>,7<sup>2</sup>,6<sup>3</sup>,5<sup>2</sup>,4<sup>3</sup>,3<sup>2</sup>,2<sup>3</sup>,1<sup>3</sup>-Octa(NH<sub>2</sub>-Glu-Leu-Glu-carbonylmethoxy)-*p*-octiphenyl (14)**: Deprotection of **17** (5.5 mg, 1.08  $\mu$ mol) by following procedure C gave pure **14** (4.5 mg, 100%) as a white solid. UV/Vis (H<sub>2</sub>O): 314 nm (28.6); <sup>1</sup>H NMR (300 MHz, CDCl<sub>3</sub>/CD<sub>3</sub>OD 1:1, 25 °C, TMS):  $\delta$  = 7.50–7.28 (m, 24H; ArH), 6.95 (d, <sup>3</sup>*J*(H,H) = 8.0, 2H; ArH), 4.82–4.20 (several m, 40H; ArOCH<sub>2</sub>, Leu-H <sub>$\alpha$</sub> , Glu-H <sub>$\alpha$</sub> ), 2.44–2.26 (m, 32H; Glu-H <sub>$\alpha$</sub> ), 2.24–1.46 (several m, 56H; Leu-H <sub>$\beta,\gamma$</sub> , Glu-H <sub>$\beta$</sub> ), 0.94–0.78 (m, 48H; Leu-CH<sub>3</sub>); <sup>1</sup>H NMR (500 MHz, D<sub>2</sub>O/CD<sub>3</sub>OD 5:1, pH = 6.4, 25 °C, TMS):  $\delta$  = 7.6–6.8 (very broad m, 26H; ArH), 4.50–4.00 (several m, 40H; ArOCH<sub>2</sub>, Leu-H, Glu-H), 2.55–2.28 (several m, 32H; Glu-H <sub>$\alpha$</sub> ), 2.20–1.40 (several m, 56H; Leu-H <sub>$\beta,\gamma$</sub> , Glu-H <sub>$\beta$</sub> ), 0.90–0.00 (very broad m, 48H; Leu-CH<sub>3</sub>); fluorescence (H<sub>2</sub>O): 314 (excitation), 385 nm (emission); CD (H<sub>2</sub>O): see Figure 4.

**8<sup>3</sup>,7<sup>2</sup>,6<sup>3</sup>,5<sup>2</sup>,4<sup>3</sup>,3<sup>2</sup>,2<sup>3</sup>,1<sup>3</sup>-Octa(NH<sub>2</sub>-Lys(Boc)-Leu-Lys(Boc)-carbonylmethoxy)-*p*-octiphenyl (16)**: Coupling of **15** (6.3 mg, 5.2  $\mu$ mol) in DMSO (1 mL, instead of CH<sub>2</sub>Cl<sub>2</sub>) and H-Lys(Boc)-Leu-Lys(Boc)-NH<sub>2</sub> (64 mg, 11  $\mu$ mol) by following procedure A, and purification of the crude product by PTLC (CH<sub>2</sub>Cl<sub>2</sub>/MeOH 10:1, *R<sub>f</sub>* = 0.1 first run, *R<sub>f</sub>* = 0.5 second run) yielded pure **16** (16.8 mg, 56%) as a white solid. <sup>1</sup>H NMR (500 MHz, CDCl<sub>3</sub>/CD<sub>3</sub>OD 1:1, 25 °C, TMS):  $\delta$  = 7.55–7.24 (m, 24H; ArH), 6.96 (d, <sup>3</sup>*J*(H,H) = 7.4 Hz, 2H; ArH), 4.80–4.20 (several m, 40H; ArOCH<sub>2</sub>, Leu-H <sub>$\alpha$</sub> , Lys-H <sub>$\alpha$</sub> ), 3.20–2.70 (m, 32H; Lys-H <sub>$\alpha$</sub> ), 1.90–1.00 (m, 120H; Leu-H <sub>$\beta,\gamma$</sub> , Lys-H <sub>$\beta,\gamma,\delta$</sub> ), 1.48–1.21 (several s, 144H; Boc-CH<sub>3</sub>), 0.94–0.75 (m, 48H; Leu-CH<sub>3</sub>); MS (ESI, MeOH, 1% formic acid): *m/z* (%): 1461.6 (94) [*M*+Na]<sup>+</sup>, 1942 (100) [*M*+Na]<sup>2+</sup>, 2896 (16) [*M*+Na]<sup>2+</sup>.

**8<sup>3</sup>,7<sup>2</sup>,6<sup>3</sup>,5<sup>2</sup>,4<sup>3</sup>,3<sup>2</sup>,2<sup>3</sup>,1<sup>3</sup>-Octa(NH<sub>2</sub>-Lys-Leu-Lys-carbonylmethoxy)-*p*-octiphenyl (13)**: Deprotection of **16** (2.6 mg, 0.35  $\mu$ mol) by following procedure C gave pure **13** (1.4 mg, 100%) as a white solid. UV/Vis (H<sub>2</sub>O): 316 nm (28.6); <sup>1</sup>H NMR (300 MHz, CDCl<sub>3</sub>/CD<sub>3</sub>OD 1:1, 25 °C, TMS):  $\delta$  = 7.55–7.22 (m, 24H; ArH), 7.00–6.90 (m, 2H; ArH), 4.80–4.20 (several m, 40H; ArOCH<sub>2</sub>, Leu-H <sub>$\alpha$</sub> , Lys-H <sub>$\alpha$</sub> ), 2.98–2.62 (m, 32H; Lys-H <sub>$\alpha$</sub> ), 1.95–1.00 (m, 120H; Leu-H <sub>$\beta,\gamma$</sub> , Lys-H <sub>$\beta,\gamma,\delta$</sub> ), 0.95–0.75 (m, 48H; Leu-CH<sub>3</sub>); <sup>1</sup>H NMR (500 MHz, D<sub>2</sub>O/CD<sub>3</sub>OD 5:1, pH = 6.4, 25 °C, TMS):  $\delta$  = 7.60–7.26 (m, 24H; ArH), 7.05 (d, <sup>3</sup>*J*(H,H) = 8.5 Hz, 2H; ArH), 4.85–4.22 (several m, 40H; ArOCH<sub>2</sub>, Leu-H <sub>$\alpha$</sub> , Lys-H <sub>$\alpha$</sub> ), 3.02–2.70 (m, 32H; Lys-H <sub>$\alpha$</sub> ), 1.90–1.10 (m, 120H; Leu-H <sub>$\beta,\gamma$</sub> , Lys-H <sub>$\beta,\gamma,\delta$</sub> ), 1.00–0.68 (m, 48H; Leu-CH<sub>3</sub>); fluorescence (H<sub>2</sub>O, pH 6.4): 316 (excitation), 385 nm (emission); CD (H<sub>2</sub>O, pH 6.4): see Figure 4.

**Rigid-rod  $\beta$ -barrels 12<sup>4</sup> (12<sup>6</sup>) (general procedure D)**: Solutions of **13** (0–32  $\mu$ mol) in MeOH (20  $\mu$ L) and/or solutions of **14** (0–32  $\mu$ mol) in MeOH (20  $\mu$ L) were added to 2.5 mL of buffer (10 mM Na<sub>2</sub>H<sub>3</sub>PO<sub>4</sub>, pH 6.4). Products were characterized by gel filtration (GF). SEC: (H<sub>2</sub>O, pH 6.4): see

Figure 3a; UV/Vis (H<sub>2</sub>O, pH 6.4): 316 nm (28.6); CD (H<sub>2</sub>O): see Figures 4 and 5; fluorescence (H<sub>2</sub>O, pH 6.4): see Figure 7c. Dependence of  $\beta$ -barrel formation on rod stoichiometry was assessed by addition of different mole fractions of **13** and **14** and subsequent measurement of the CD spectra (Figure 5a). Dependence of  $\beta$ -barrel formation on ionic strength (0–1M NaCl) and pH (pH 2–12) was assessed with correspondingly changed buffers (Figures 1 5a and c).  $\beta$ -Barrel stability was assessed by heating the water-jacketed CD-cell and by sample dilution with continuous measurement of the CD spectra (not shown).

**Rigid-rod  $\beta$ -barrels 12<sup>a</sup> (12<sup>b</sup>) (general procedure E):** Identical concentrations of **13** and **14** were dissolved in MeOH/chloroform, and sodium cholate (64.5 mg, 0.15 mmol) and increasing amounts of MeOH/chloroform were added until a clear solution was obtained. The organic solvents were slowly evaporated at RT, and the resulting film was dried for at least 2 h in vacuo. Then Na<sub>n</sub>H<sub>3–n</sub>PO<sub>4</sub> (10 mM, 1.0 mL, pH 6.4) was added. Hydration of the resulting suspension was eventually accelerated by sonication or heating. The mixed micellar mixture was filtered through cotton. This micellar mixture (1 mL) was then dialyzed 12 times against buffer (1 mL) for > 2 h at RT in the dark by using dialysis cells (Fisher) with membranes from Diachem (MW-cutoff = 5000) mounted on a Thermomixer (Fisher) shaking at about 1300 rpm. The resulting mixture was filtered twice through cotton and characterized by gel filtration (GF). SEC: (H<sub>2</sub>O, pH 6.4): see Figure 3a; UV/Vis (H<sub>2</sub>O, pH 6.4): 316 nm (28.6); CD (H<sub>2</sub>O): see Figure 4; fluorescence (H<sub>2</sub>O, pH 6.4): see Figure 7b.

**Rigid-rod  $\beta$ -barrels 12<sup>n</sup> (general procedure F):** Identical concentrations of **13** and **14** were dissolved in MeOH/chloroform, and *n*-octyl  $\beta$ -D-glucopyranoside (36.5 mg, 125  $\mu$ mol) and increasing amounts of MeOH/chloroform were added until a clear solution was obtained. The organic solvents were slowly evaporated at RT, the resulting film was dried for at least 2 h in vacuo. Then Na<sub>n</sub>H<sub>3–n</sub>PO<sub>4</sub> (10 mM, 1.0 mL, pH 6.4) was added. Hydration of the resulting suspension was eventually accelerated by sonication or heating. The mixed micellar mixture was filtered through cotton. This micellar mixture (1 mL) was then dialyzed once against buffer (1 L) for > 2 h at RT in the dark by using Mini Lipoprep<sup>®</sup> (Sialomed) with the dialysis chamber rotating at 20 rpm. The resulting mixture was filtered twice through cotton and characterized by gel filtration (GF). SEC: (H<sub>2</sub>O, pH 6.4): see Figure 3d; UV/Vis (H<sub>2</sub>O, pH 6.4): 2781 nm (24.0). CD (H<sub>2</sub>O, pH 6.4): 288 nm (–2.3).

**Rigid-rod lipocalin 19:** By following procedure E,  $\beta$ -carotene **11**, **13**, and **14** (molar ratio = 1:0.5:0.5) were assembled to give **19** in 25% yield with respect to **11** and 100% yield with respect to **13** and **14** (Table 1, entry 1). Carotenolipocalin **19** was characterized by gel filtration (GF). SEC: (H<sub>2</sub>O, pH 6.4): see Figure 3e; UV/Vis (H<sub>2</sub>O, pH 6.4): see Figure 7b; CD (H<sub>2</sub>O, pH 6.4): see Figure 7a; fluorescence (H<sub>2</sub>O, pH 6.4): see Figure 7c. Control experiments: a) excess  $\beta$ -carotene (1:0.1:0.1) gave about identical results; b) excess rods (1:2.5:2.5): < 5% yield; c) without **13** (1:0:1): < 5% yield; d) without **13** and **14** (1:0:0): < 5% yield.

**Rigid-rod disc micelle 20:** By following procedure E, astaxanthin **10**, **13**, and **14** (molar ratio = 1:0.1:0.1) were assembled to give **20** in 10% yield with respect to **10** and about 50% yield with respect to **13** and **14** (Table 1, entry 9). Disc micelles **20** were characterized by gel filtration (GF). SEC: (H<sub>2</sub>O, pH 6.4): MW  $\approx$  84000 (not 100% reproducible); UV/Vis (H<sub>2</sub>O, pH 6.4): see Figure 9; CD (H<sub>2</sub>O, pH 6.4): 602 (+46), 442 nm (–38); fluorescence (H<sub>2</sub>O, pH 6.4): 316 (excitation), 385 nm (emission, 29% quenching). Control experiments: a) excess rods (1:1:1) gave about identical results; b) without rods (1:0:0): 17% yield; GF (H<sub>2</sub>O, pH 6.4): not eluted; SEC: (H<sub>2</sub>O, pH 6.4): not eluted; UV/Vis (H<sub>2</sub>O, pH 6.4): see Figure 9; CD (H<sub>2</sub>O, pH 6.4): 572 (–46), 424 nm (+64); fluorescence (H<sub>2</sub>O, pH 6.4): 316 (excitation), 385 nm (emission); c) without **13** (1:0:0.2): 6% yield; data as in b; d) without **14** (1:0.2:0): < 5% yield. Control experiments with carotenoids **9** and **18** were performed by following procedure E (see Table 1, entries 4–8).

## Acknowledgement

We are grateful to Dr. N. Majumdar for synthesizing **15**, and to Dr. A. C. de Dios for measurement of 500 MHz NMR spectra. We thank NIH (GM56147), Research Corporation (Research Innovation Award), Sundry Institute for Bioorganic Research (SUNBOR Grant), Georgetown Uni-

versity, and the University of Geneva for support of this work. Further support by NSF (CHE-9601976) through the Georgetown Molecular Modeling Center is gratefully acknowledged. Mass spectrometry was performed by Dr. N. Leffers at Georgetown University Lombardi Cancer Center's Macromolecular Analysis Shared Resource, which is supported in part by U.S. PHS Grant P30-CA-51008, and by Dr. K. Lu and C. Ladd at University of Maryland, College Park.

- a) K. K. Kim, R. Kim, S.-H. Kim, *Nature* **1998**, *394*, 595; b) A. L. Horwich, H. R. Saibil, *Nat. Struct. Biol.* **1998**, *5*, 333; c) L. Ditzel, J. Löwe, D. Stock, K.-O. Stetter, H. Huber, R. Huber, S. Steinbacher, *Cell* **1998**, *93*, 125; d) B. Bukau, A. L. Horwich, *Cell* **1998**, *92*, 351.
- a) W. Baumeister, J. Walz, F. Zühl, E. Seemüller, *Cell* **1998**, *92*, 367; b) J. Löwe, D. Stock, B. Jap, P. Zwickl, W. Baumeister, R. Huber, *Science* **1995**, *268*, 534.
- a) L. Joshua-Tor, H. E. Xu, S. A. Johnston, D. C. Rees, *Science* **1995**, *269*, 945; b) T. S. R. Krishna, X.-P. Kong, S. Gary, P. M. Burgers, J. Kuriyan, *Cell* **1994**, *79*, 1233; c) C. D. Lima, J. C. Wang, A. Mondragon, *Nature* **1994**, *367*, 138; d) X.-P. Kong, R. Onrust, M. O'Donnell, J. Kuriyan, *Cell* **1992**, *69*, 425; e) D. B. Nikolov, S.-H. Hu, J. Lin, A. Gasch, A. Hoffmann, M. Horikoshi, N.-H. Chua, R. G. Roeder, S. K. Burley, *Nature* **1992**, *360*, 40.
- T. A. Baker, S. P. Bell, *Cell* **1998**, *92*, 295.
- a) L.-Q. Gu, O. Braha, S. Conlan, S. Cheley, H. Bayley, *Nature* **1999**, *398*, 686; b) C. Lesieur, B. Vécsey-Semjén, L. Abrami, M. Fivaz, F. G. van der Goot, *Mol. Membrane Biol.* **1997**, *14*, 45; c) L. Song, M. R. Hobaugh, C. Shustack, S. Cheley, H. Bayley, J. E. Gouaux, *Science* **1996**, *274*, 1859; d) T. Schirmer, T. A. Keller, Y.-F. Wang, J. P. Rosenbusch, *Science* **1995**, *267*, 512; e) S. R. Durell, H. R. Guy, N. Arispe, E. Rojas, H. B. Pollard, *Biophys. J.* **1994**, *67*, 2137; f) M. S. Weiss, A. Kreusch, E. Schiltz, U. Nestel, W. Welte, J. Weckesser, G. E. Schulz, *FEBS Lett.* **1991**, *280*, 379.
- a) G. Beste, F. S. Schmidt, T. Stibora, A. Skerra, *Proc. Natl. Acad. Sci. USA* **1999**, *96*, 1898; b) D. R. Flower, *Biochem. J.* **1996**, *318*, 1; Compare also: c) M. Ormö, A. B. Cubitt, K. Kallio, L. A. Gross, R. Y. Tsien, S. J. Remington, *Science* **1996**, *273*, 1392.
- a) R. C. Bugos, A. D. Hieber, H. Y. Yamamoto, *J. Biol. Chem.* **1998**, *273*, 15321; b) K. K. Niyogi, O. Björkman, A. R. Grossman, *Proc. Natl. Acad. Sci. USA* **1997**, *94*, 14162; c) H. A. Frank, R. J. Cogdell, *Photochem. Photobiol.* **1996**, *63*, 257; d) Y. Koyama, M. Kuki, P. O. Anderson, T. Gillbro, *Photochem. Photobiol.* **1996**, *63*, 243.
- a) G. Britton, R. J. Weesie, D. Askin, J. D. Warburton, L. Gallardo-Guerrero, F. J. Jansen, H. J. M. de Groot, J. Lugtenburg, J.-P. Cornard, J. C. Merlin, *Pure Appl. Chem.* **1997**, *69*, 2075; b) P. F. Zagalsky, *Pure Appl. Chem.* **1994**, *66*, 973; c) J. N. Keen, I. Caceres, E. E. Eliopoulos, P. F. Zagalsky, J. B. C. Findlay, *Eur. J. Biochem.* **1991**, *202*, 31; d) R. J. H. Clark, N. R. D'Urso, P. F. Zagalsky, *J. Am. Chem. Soc.* **1980**, *102*, 6693.
- a) M. Z. Papiz, L. Sawyer, E. E. Eliopoulos, A. C. T. North, J. B. C. Findlay, R. Sivaprasadarao, T. A. Jones, M. E. Newcomer, P. J. Kraulis, *Nature* **1986**, *324*, 383; b) R. Hemley, B. E. Kohler, P. Siviiski, *Biophys. J.* **1979**, *28*, 447; c) S. Futterman, J. Heller, *J. Biol. Chem.* **1972**, *247*, 5168.
- N. Sakai, N. Majumdar, S. Matile, *J. Am. Chem. Soc.* **1999**, *121*, 4294.
- a) S. R. LaBrenz, J. W. Kelly, *J. Am. Chem. Soc.* **1995**, *117*, 1655; b) J. P. Schneider, J. W. Kelly, *Chem. Rev.* **1995**, *95*, 2169; For "non-rigid-rod" scaffolds, see: c) J. S. Nowick, *Acc. Chem. Res.* **1999**, *32*, 287.
- a) B. Baumeister, A. C. de Dios, S. Matile, *Tetrahedron Lett.* **1999**, *40*, 4623; b) B. Ghebremariam, S. Matile, *Enantiomer* **1999**, *4*, 121; B. Ghebremariam, S. Matile, *Enantiomer* **1999**, *4*, 131 (A. M. Rouhi, *Chem. Eng. News* **1999**, *77*(22), 32); c) M. M. Tedesco, B. Ghebremariam, N. Sakai, S. Matile, *Angew. Chem.* **1999**, *111*, 523; *Angew. Chem. Int. Ed.* **1999**, *38*, 540; d) N. Sakai, C. Ni, S. M. Bezrukov, S. Matile, *Bioorg. Med. Chem. Lett.* **1998**, *8*, 2743; e) C. Ni, S. Matile, *Chem. Commun.* **1998**, 755; f) L. A. Weiss, N. Sakai, B. Ghebremariam, C. Ni, S. Matile, *J. Am. Chem. Soc.* **1997**, *119*, 12142; g) N. Sakai, K. C. Brennan, L. A. Weiss, S. Matile, *J. Am. Chem. Soc.* **1997**, *119*, 8726; excellent reviews on synthesis and properties of rigid-rod molecules have appeared very recently: h) P. F. H. Schwab, M. D. Levin, J. Michl, *Chem. Rev.* **1999**, *99*, 1863; i) A. J. Berresheim, M. Müller, K. Müllen,

- Chem. Rev.* **1999**, *99*, 1747; j) R. E. Martin, F. Diederich, *Angew. Chem.* **1999**, *111*, 1440; *Angew. Chem. Int. Ed.* **1999**, *38*, 1351; k) N. Sakai, S. Matile, *Chem. Eur. J.* **2000**, *6*, 1731.
- [13] H. Torii, M. Tasumi, *J. Chem. Phys.* **1993**, *98*, 3697, and references cited therein.
- [14] a) J. L. Haley, A. N. Fitch, C. Lambert, T. G. Truscott, J. N. Chacon, D. Stirling, W. Schalch, *J. Chem. Soc. Chem. Commun.* **1992**, 1175; b) G. C. Chen, M. Krieger, J. P. Kane, C.-S. C. Wu, M. S. Brown, J. L. Goldstein, *Biochemistry* **1980**, *19*, 4706; c) H. Y. Yamamoto, A. D. Bangham, *Biochim. Biophys. Acta* **1978**, *507*, 119.
- [15] a) P. O. Anderson, S. M. Bachilo, R. L. Chen, T. Gillbro, *J. Phys. Chem.* **1995**, *99*, 16199; b) S. L. Bondarev, S. M. Bachilo, S. S. Dvornikov, S. A. Tikhomirov, *J. Photochem. Photobiol. A* **1989**, *46*, 315.
- [16] K. Gaier, A. Angerhofer, A. C. Wolf, *Chem. Phys. Lett.* **1991**, *187*, 103.
- [17] R. Hemley, B. E. Kohler, *Biophys. J.* **1977**, *20*, 377.
- [18] A. Milon, G. Wolff, G. Ourisson, Y. Nakatani, *Helv. Chim. Acta* **1986**, *69*, 12, and references cited therein.
- [19] H. Houjou, Y. Inoue, M. Sakurai, *J. Am. Chem. Soc.* **1998**, *120*, 4459, and references cited therein.
- [20] a) D. Ranganathan, C. Lakshmi, I. L. Karle, *J. Am. Chem. Soc.* **1999**, *121*, 6105; b) J. D. Hartgerink, T. D. Clark, M. R. Ghadiri, *Chem. Eur. J.* **1998**, *4*, 1367; c) T. D. Clark, L. K. Buehler, M. R. Ghadiri, *J. Am. Chem. Soc.* **1998**, *120*, 651; d) D. Seebach, J. L. Matthews, A. Meden, T. Wessels, C. Baerlocher, L. B. McCusker, *Helv. Chim. Acta* **1997**, *80*, 173; e) K. Benner, P. Klüfers, J. Schuhmacher, *Angew. Chem.* **1997**, *109*, 783; *Angew. Chem. Int. Ed. Engl.* **1997**, *36*, 743; f) G. Gattuso, S. Menzer, S. A. Nepogodiev, J. F. Stoddart, D. J. Williams, *Angew. Chem.* **1997**, *109*, 1615; *Angew. Chem. Int. Ed. Engl.* **1997**, *36*, 1451; g) D. Venkataraman, S. Lee, J. Zhang, J. S. Moore, *Nature* **1994**, *371*, 591; h) X. C. Sun, G. P. Lorenzi, *Helv. Chim. Acta* **1994**, *77*, 1520; i) A. Harada, J. Li, M. Kamachi, *Nature* **1993**, *364*, 516; j) I. L. Karle, B. K. Handa, C. H. Hassall, *Acta Crystallogr. Sect. B* **1975**, *31*, 555.
- [21] J. Coste, D. Le-Nguyen, B. Castro, *Tetrahedron Lett.* **1990**, *31*, 205.
- [22] Structural studies of **12<sup>4</sup>** (**12<sup>6</sup>**) were thus restricted to techniques more sensitive than 500 MHz <sup>1</sup>H NMR, <sup>13</sup>C NMR and IR spectroscopy. Supramolecules **12<sup>4</sup>** (**12<sup>6</sup>**) were also not detectable with confidence by ESI-MS.
- [23] a) D. V. Waterhous, W. C. Johnson, Jr., *Biochemistry* **1994**, *33*, 2121; b) L. Zhong, W. C. Johnson, Jr., *Proc. Natl. Acad. Sci. USA* **1992**, *89*, 4462; c) D. S. Yang, C. C. Wu, H. M. Martinez, *Methods Enzymol.* **1986**, *130*, 208.
- [24] a) L. V. Najbar, D. J. Craik, J. D. Wade, D. Salvatore, M. McLeish, *Biochemistry* **1997**, *36*, 11525; b) M. C. Manning, M. Illangasekare, R. W. Woody, *Biophys. Chem.* **1988**, *31*, 77.
- [25] a) J. Reed, T. A. Reed, *Anal. Biochem.* **1997**, *254*, 36; b) D. W. Choo, J. P. Schneider, N. R. Graciani, J. W. Kelly, *Macromolecules* **1996**, *29*, 355; c) A. Brack, G. Spach, *J. Am. Chem. Soc.* **1981**, *103*, 6319; d) P. K. Sarkar, P. Doty, *Proc. Natl. Acad. Sci. USA* **1966**, *55*, 901.
- [26] K. A. Connors, *Binding Constants*, Wiley, New York, **1987**, p. 61.
- [27] J.-H. Fuhrhop, J. Köning, *Membranes and Molecular Assemblies: The Cytokinetic Approach*, The Royal Society of Chemistry, Cambridge (UK), **1994**.
- [28] For comparison of toroidal with the widely studied spherical capsules, see, for example: a) J. Rebek, Jr., *Acc. Chem. Res.* **1999**, *32*, 278; b) L. R. MacGillivray, J. L. Atwood, *Angew. Chem.* **1999**, *111*, 1080; *Angew. Chem. Int. Ed. Engl.* **1999**, *38*, 1018; c) A. Jasat, J. C. Sherman, *Chem. Rev.* **1999**, *99*, 931; d) J. de Mendoza, *Chem. Eur. J.* **1998**, *4*, 1373; e) T. Douglas, M. Young, *Nature* **1998**, *393*, 152; f) R. Warmuth, *Angew. Chem.* **1997**, *109*, 1406; *Angew. Chem. Int. Ed. Engl.* **1997**, *36*, 1347.
- [29] C. E. Dempsey, *Biochim. Biophys. Acta* **1990**, *1031*, 143, and references cited therein.
- [30] T. Goto, T. Kondo, *Angew. Chem.* **1991**, *103*, 17; *Angew. Chem. Int. Ed. Engl.* **1991**, *30*, 17.
- [31] a) S. J. Wiczorek, K. A. Kalivoda, J. G. Clifton, D. Ringe, A. Petsko, J. A. Gerlt, *J. Am. Chem. Soc.* **1999**, *121*, 4540; b) M. Henning, A. D'Arcy, I. C. Hampele, M. P. G. Page, *Nature Struct. Biol.* **1998**, *5*, 357; c) P. C. Babbitt, J. A. Gerlt, *J. Biol. Chem.* **1997**, *272*, 30591.

Received: August 2, 1999 [F1955]